Università
Ca'Foscari
Venezia

Master's Degree Programme

Environmental Sciences

Global Environmental Change

Final Thesis

Climate-related variability of isotopic records in a coastal Antarctic ice core

Supervisor
Prof. Barbara Stenni

Assistant supervisor
Giuliano Dreossi
Research Associate

Master's Student
Ishaq Khan
860758

Academic Year
2018 / 2019

Abstract

Polar ice cores, both in Greenland and Antarctica, provide an improved understanding of past climatic variations through $\delta^{18}O$ and δD records, which are considered a proxy of surface temperature. This study focusses on the isotopic records obtained from four ice cores drilled in a coastal site of East Antarctica (GV7), characterized by a relatively high snow accumulation rate (237 mm of water equivalent). At this site different cores have been retrieved, one of which reached a depth of 250 m, while others reached shallow (5-12 m) or intermediate (55 m) depths, covering different time periods; this allows to calculate a stacked record for this site, in order to reduce the stratigraphic noise. The co-isotopic analysis allows the definition of the deuterium excess ($d=\delta D-8*\delta^{18}O$), which is a proxy of climatic conditions (relative humidity, sea surface temperature and wind speed) in the moisture source regions of precipitation. Since the isotopic records are not only related to temperature but also to other factors (precipitation intermittency, snow redistribution by winds and post-depositional effects), we compare the mean annual GV7 values of $\delta^{18}O$, δD, d and snow accumulation rate, all of which determined after an annual layer dating approach, to re-analysis data over the 1979-2012 period. For validating the proxy records, we used the ERA-Interim reanalysis data of temperature and precipitation, as well as the ECHAM5-wiso model data, which includes also the stable isotopes. We found that ERA-Interim over-estimates the precipitation data at GV7, which is already known in literature in coastal areas of Antarctica, while the ECHAM5-wiso under-estimates them. The simulated temperature data from ECHAM5-wiso were found in strong agreement with stable isotopes from GV7 ice cores, when using a 3-year moving average, apart from one of them. Furthermore, we also compared the d-excess records with sea ice extent, finding a contrasting behavior in the most recent period. We also investigated the snow accumulation records in relation to simulated temperature, finding an agreement between the two variables from 1979 to 1996, while they appear not correlated afterwards. The main climatic indices for the Southern Hemisphere, El Niño 3.4 and the Antarctic Oscillation, were also compared to stable isotopes and simulated temperatures. The overall model-data comparison in this study and for this area shows a relatively good agreement, both in terms of absolute values and variability.

Acknowledgement

First and foremost, I would like to thank my supervisor Professor Barbara Stenni. During this research, she has consistently motivated me to produce originality in my work. She has always prompted me to dedicate myself to attain my goals. It is worth mentioning that Barbara Stenni has made me able to enrich my skills through her insights in the field of paleoclimatology, which in turn, has steered me in the right direction. I believe that this work has made a small contribution to existing studies in this field.

I am equally indebted to my co-supervisor Giuliano Dreossi (Research Associate). I highly appreciate him for his welcoming attitude and the courage he has given me. Whenever I have found myself directionless, he has wholeheartedly helped me to resolve my problems. Undoubtedly, my work would have been incomplete if he had not taught me some of the critical aspects of this work. His mentorship not only made my work complete but would help in my further studies in this field.

I would also like to acknowledge the services of Professor Dario Battistel whose teaching enabled me to pursue my research in the field of paleoclimatology. I thank him for referring me to Professor Barbara Stenni with whom I completed my final thesis.

Last but not the least, I must express my profound gratitude to my parents, brothers, and my friends Syed Asif Ali Shah and Sarah El Ouarti, for their unfailing support and encouragement throughout the period of my studies. I would not have been able to attain this accomplishment without their kind support.

CONTENTS

1. Introduction and Objectives

The Earth's climate has been through variations from the very start of its existence. For the last 4.6 billion years, Earth's climate went through swings of stability, calm and extreme variations (Quante, 2010). The climate is a complex and interactive system consisting of different components, e.g., atmosphere, land surface, ocean and other water bodies, snow and ice cover, and living things. Climate is usually described as the average temperature, precipitation, and wind over a period (the classical period is 30 years) ranging from few months to millions of years (IPCC.ch, 2019). According to physical principles, some trace gases in the atmosphere such as CO_2 and water vapor restrict the radiant flow of heat from Earth to space and this mechanism is known as the "greenhouse effect", which already makes the Earth's surface and lower atmosphere warmer than they would be without greenhouse gases. According to the International Panel on Climate Change (IPCC), the anthropogenic greenhouse gases emissions of the industrial period are unprecedented and have caused an increase of about 1°C in the average temperature of the Earth's surface (IPCC Special Report, 2018), associated with a 19 cm rise in sea level from 1901 to 2010 (IPCC AR5, 2013). The observed interannual and decadal variations for the last 15 years in Earth's surface temperature have been found associated with El Niño Southern Oscillation (ENSO) events (Muller et al., 2013). If we come to the most recent update of average global temperature, 2016 was the warmest year on record (NOAA, 2017) triggered by an exceptionally strong ENSO event (Anyambe et al., 2019). El Niño can enhance warming but it is not the sole cause of the recent year temperature records: 2017 and 2018 were the third and the fourth warmest years on record, respectively, without El Niño events (Climate Central., 2019).

1.2 Recent Past Climate Changes in Antarctica

Antarctica is an area of particular interest for climate studies due to i) the so-far poor understanding of the interactions between the different components of its climate system, ii) the amplification of climate changes compared to low latitudes, iii) it's strong regional variability. The Antarctic ice sheet is also the main reservoir of freshwater on Earth (around 90%) and its projected future partial melting, due to increasing temperatures, could substantially increase the sea level worldwide (IPCC, 2019).

Instrumental observations in Antarctica, with few exceptions, started only during the 1957-58 International Geophysical Year, with most of the weather stations placed in coastal areas. The Antarctic Peninsula is the sector characterized by the longest instrumental records, starting from the late 1940s (King and Turner, 1997); both instrumental and proxy records show a warming trend in this region, which has started during the first half of 1900s (Thomas et al., 2009). The highest increase has been observed in the western and northern Antarctic Peninsula (Turner et al., 2014), with the record belonging to the Faraday/Vernadsky station, which registered an increment of +0.54°C per decade for the 1951-2011 period. The Peninsula warming is also coupled with an increase in precipitation (Thomas et al., 2008), although the warming rate over the Peninsula has slowed during the last 10-15 years (fig 1.2.1) (Jones et al., 2016).

Even West Antarctica has been characterized by a significant warming starting from the 1950s (at Byrd Station an increase of 2.2 ± 1.3 °C was observed between 1958 and 2010; Bromwich et al., 2014).

Both coastal and inland East Antarctica have not yet showed any statistically significant temperature trend in the instrumental era, with the Epica Dronning Maud Land (EDML) and the Talos Dome ice core isotopic records displaying a warming and a cooling trend, respectively, over the last 100 years (Thomas et al., 2016).

Paleotemperature reconstructions derived from proxies are thus of crucial importance in order to understand even recent climatic variations in the continent, and only ice core isotopic records can provide a sub-decadal resolution for temperature change reconstructions (Küttel et al., 2012).

Since 1979 satellite observations have significantly improved the knowledge of the Antarctic climate, although satellite sensor changes led to uncertainties regarding the different acquired datasets (Eisenman

et al., 2014).

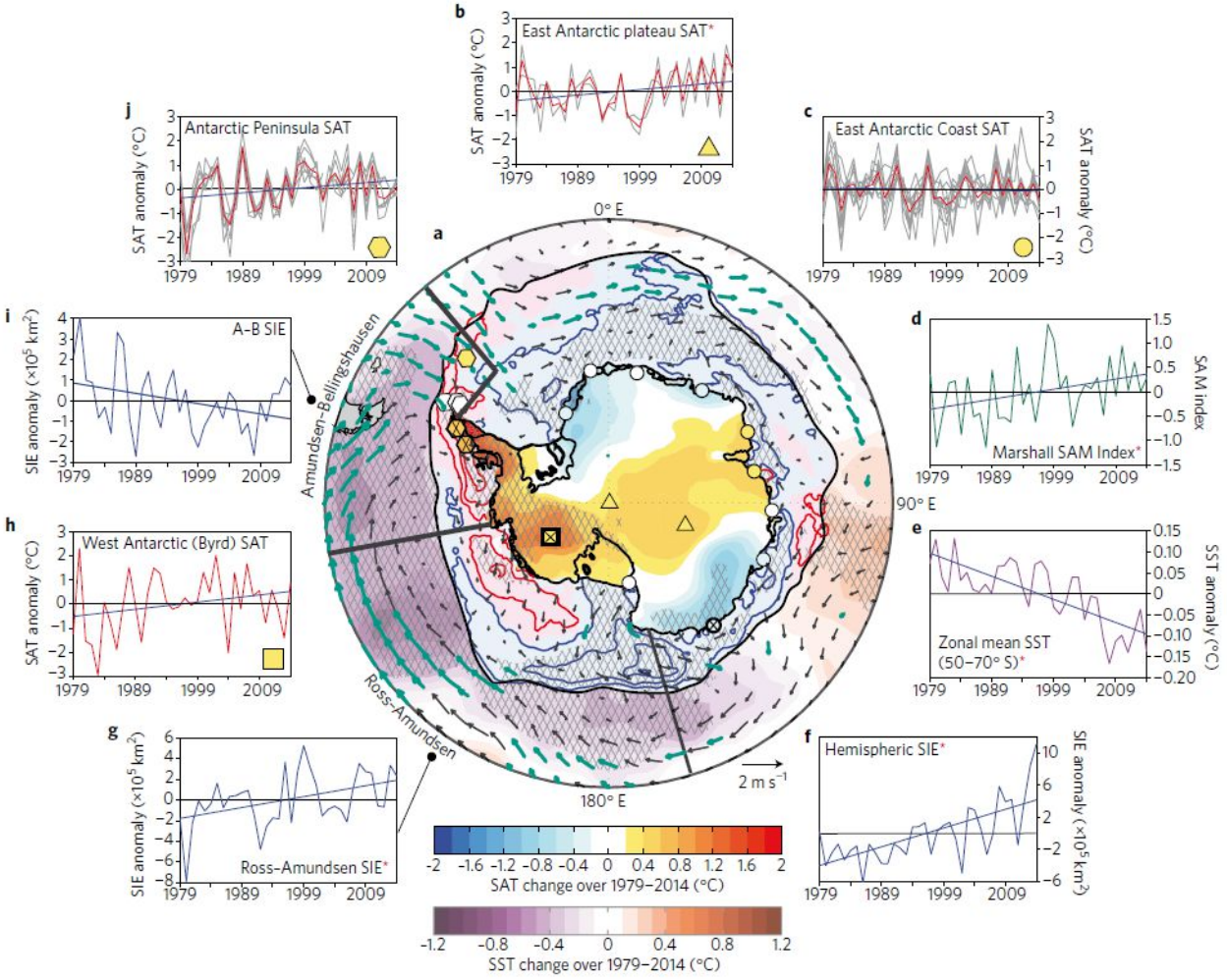

Fig.1.2.1- Total changes in the mean annual surface air temperature (blue-red shading), station-based air temperature (SAT, blue red-shaded shapes), sea-ice extension (red and blue contours , alongside light pink and blue shading beneath denote negative and positive trend respectively), sea surface temperature and 10-m wind (denoted with purple red shading and vectors respectively) over a period of 1979-2014. Source: (Jones et al., 2016).

1.3 Proxy data and its significance

Paleoenvironmental sciences adopt different methodologies to observe, describe, and understand Earth's system processes and how they evolved through times. A paleoenvironmental archive locks-in and preserves information of various Earth's components through various times scales. The proxies contained in these natural archives can also be described as "the indirect measure of the variable that cannot be directly measured". There are different natural archives for retrieving past information such as coral reef for reconstructing sea-level variations; marine sediments, consisting of biogenic and terrigenous materials

for revealing past sea surface temperature, sea ice variability, ice volume and oceanic circulation; pollen, which reconstructs vegetation history in the past and ice cores for retrieving the paleotemperature and hydrological cycle. The research work carried out in this thesis focusses on the study of recent past climatic changes through ice cores.

1.4 Why ice cores?

Ice cores are long cylindrical-shaped ice pieces, drilled out from ice sheets in Polar Regions as well as in low-latitude high-altitude regions, reaching different depths, ranging from a few meters to 3 km. Ice sheet and glacier formation starts from snow accumulation turning into firn and subsequently into ice. Pores in the ice cores decrease with increasing depth and with the weight of the overlying snow. Remaining air bubbles are thus trapped in the ice below the firn-ice transition, holding past atmospheric gases, while the different ice layers from top to bottom constitute an increasing timescale. Ice cores also provide the number of dust records in the atmosphere, which considered to be associated with the very dry and windy climatic conditions. During volcanic eruptions, tiny ash particles are released in the atmosphere and transported with air masses that drop out and are trapped in the snow layers (tephra). At the same time, the SO_2 released during strong volcanic eruptions is oxidized in the atmosphere to sulphate and then deposited on ice sheets both via dry and wet depositions. These volcanic sulphate and ash layers are used as stratigraphic reference horizons that can be used for constraining the timescale of ice cores. Ice core-specific chronology depends on the thickness of the ice and to the snow accumulation rate, as well as on the thinning of the ice layers; with the overlying weight of the ice column, in the deep part of ice cores, the layers become thin, stretched and deformed.

The accumulation of snowfall on the high latitude and altitude of the Earth's surface provides extensive spatial and temporal records of the paleoenvironmental and paleoclimatic conditions (Raymond, 2014). Antarctica and Greenland are the most favorable locations for ice core drilling because of the considerable size and thickness of their ice sheets. Volume and time constant of Antarctic and Greenland ice sheets makes them the slowest component of the climate system (Masson-Delmotte., 2006).

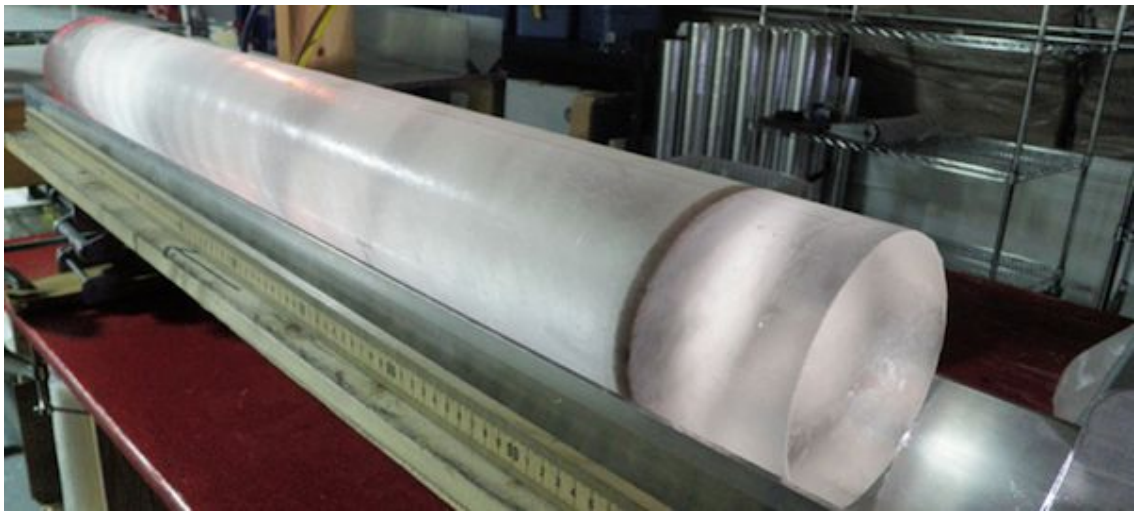

Fig 1.4.1- Ice core with distinct annual layers including tephra layer (National Science Foundation)

The oldest ice cores were recovered from Dome C (EPICA) and Dome F with a temporal extension of 810 kyr BP and 740 kyr BP, respectively. With the advancement of technology and the need for predictions of future climatic conditions, ice coring has become an integral part of climate studies. In the figure below the main drilling projects in Greenland and Antarctica are illustrated.

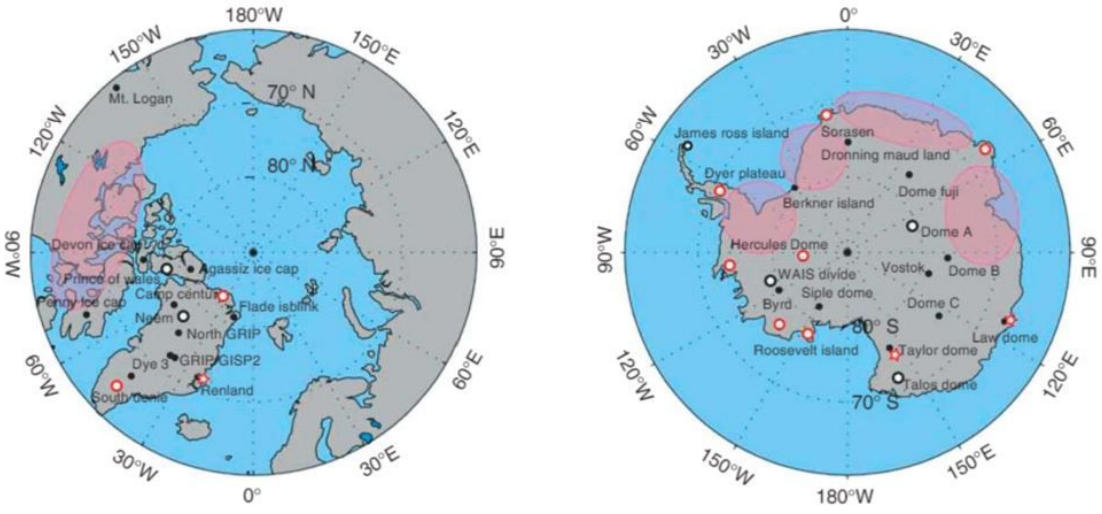

Fig 1.4.2- Greenland and Antarctic deep drilling sites (Jouzel et al., 2010). Filled circles, open black circles and red and star circles indicates already done drilling, ongoing drilling, and future projects, respectively.

1.5 Variability of $\delta^{18}O$ and δD in coastal Antarctica

Oxygen and hydrogen isotopic contents of ice cores are some of the most used proxies for reconstructing past temperatures (Jouzel et al., 2003, Hou et al., 2012). Although the isotopic contents from Vostok and EPICA Dome C ice cores were used to reconstruct the temperature for the past 400 ka and 800 ka BP (before present), respectively, yet the compilation of spatial and temporal distribution of these isotopic contents across Antarctica has remained a challenging task. Previously, various studies (e.g Lorius and Merlivat, 1977; Morgan, 1982) on compiling the database of isotopic contents spatial distribution have been conducted. More recently, Masson-Delmotte et al. (2008), updated the database from snowfall, surface snow, snow pits, and shallow firn cores and concluded that isotopic contents in snow happened to deplete from mid-latitudes to high latitudes. It was demonstrated that isotopic contents decline from coastal Antarctica to inland Antarctica and showed also a decreasing trend with increasing elevation (Hou et al., 2012). Moreover, the simulated data from (AGCM) confirmed that latitudinal, altitudinal and continental effects play a key role in the variability of isotopic contents of precipitation across Antarctica. The distribution of stable isotopes across Antarctica is highly associated with the condensation temperature (Stenni et al., 2016, Masson-Delmotte et al., 2008). Besides, several other factors such as moisture origin, seasonality/intermittency of precipitation and the post-depositional processes might pose a large uncertainty while studying water stable isotope contents from ice cores (Hou et al., 2012). Antarctic regions with a high accumulation rate are the most suitable places to obtain well-preserved signals of water stable isotopes in ice cores.

1.6 Research Objectives

This research project was funded by the Italian National Antarctic Research Program (PNRA), in association with the Korean Polar Research Institute (KOPRI). This research activity was carried out in the frame of the IPICS-2kyr-project (International Partnership for Ice Core Science, reconstructing the climate variability for the last 2kyr, the Italian contribution) (Caiazzo et al., 2017).

The main objectives of this thesis are the following;

- We aim to understand the recent inter-annual variabilities (1979-2012) of isotopic contents in a coastal area of Antarctica, which is characterized by a high snow accumulation rate, and the possible drivers of these variations.
- We aim to understand the relationships among the isotopic records from GV7 ice cores and between those records and the accumulation derived from the annual layer identification.
- We aim to assess the robustness and representativeness of model simulations for the GV7 site. We will perform a comparison between ice cores data and data derived from state-of-the-art Atmospheric General Circulation Models (AGCM), to illustrate the regional and local climatic changes in this part of Antarctica.
- We aim to investigate the influence of large-scale atmospheric phenomena such as ENSO and SAM, which play a crucial role in the climate of Antarctica, by relating the isotopic and the accumulation records from GV7 ice cores, as well as the AGCM data, to these indices over the 1979-2012 period.
- We aim to compare the GV7 ice core isotopic and accumulation records, together with temperature, precipitation and isotope data from AGCM, to sea ice extent variations over different Antarctic sea sectors. Changes (loss or gain) in the sea ice extent can cause large variations in the precipitation reaching from coastal to inland Antarctic plateau.

2 Study Area

This work is focused on Northern Victoria land and Eastern Wilkes land (East Antarctica) sector, where the drilling site, GV7 (70°41'S, 158°52'E, elevation: 1950 m a.s.l.), is located. GV7 is on the North-South transect following the ice divide extending from Oates coast to Talos Dome (Caiazzo et al., 2017). This part of eastern coastal Antarctica is characterized by a relatively high snow accumulation rate, equal to 242 ± 71 mm w. e. for the period 2008-2013 (Caiazzo et al., 2017), which is 3 times higher than Talos Dome and 10 times higher than Dome C (the area from where the oldest ice core of 800 kyr was retrieved).

Considering its high accumulation rate, the GV7 site was proposed as a potential site for retrieving ice cores of high resolution, potentially providing continuous records of climate and environmental variability over the last millennium (Becagli et al., 2004, Proposito and Frezzotti, 2008).

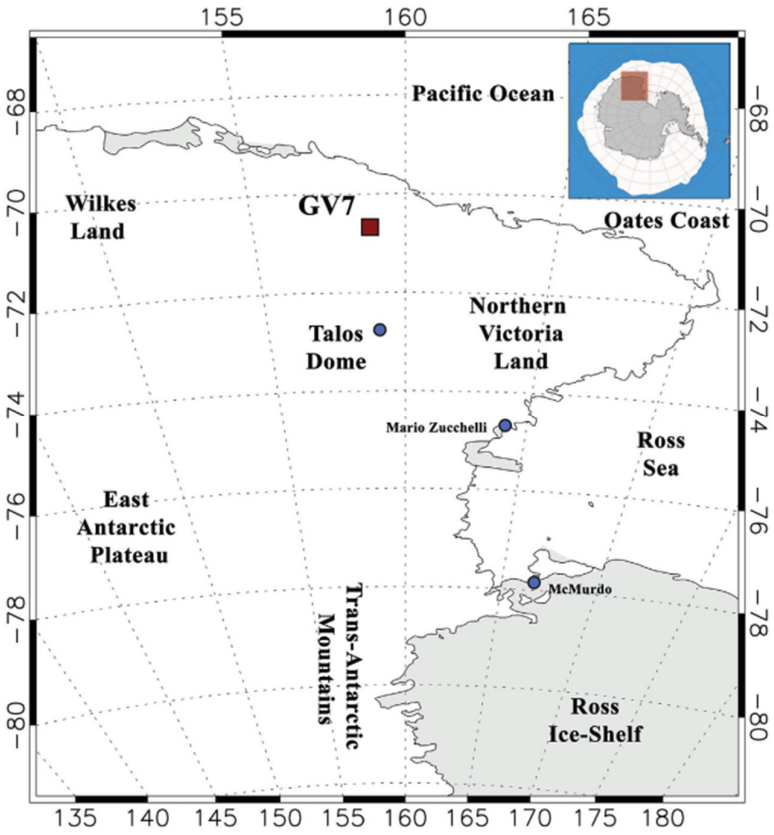

Fig 2.1- Map of Antarctica with the GV7 site spotted.

2.1 Air mass backward trajectories analysis

The backward trajectories for the GV7 site have been generated through the Hybrid Single-Particle Lagrangian Integrated Trajectory (HYSPLIT) model developed by NOAA and Australia's Bureau of Meteorology (Draxler and Rolph, 2012), for the period spanning from 2007 to 2012. HYSPLIT model calculated back trajectories for four main sectors (PLATEAU, Western Pacific Ocean-WPO, Indian Ocean - IO and Ross sea sector - RSS) arriving at the GV7 site. These analyses have been performed and reported by Caiazzo et al. (2017).

As illustrated in fig 2.1.1, GV7 receives different trajectories during 2007-2013. The highest number of trajectories, 32 %, and 29 %, originates from the Indian Ocean Sector and the Antarctic Interior (plateau area), respectively, followed by the Ross Sea Sector (21 %) and the Western Pacific Ocean (19 %). The annual averaged cumulated snow at GV7 site during 2007-2013 suggests that although the Western Pacific Ocean originates the lowest number of trajectories, yet the air masses originating from WPO are associated with highest value (147 mm) of annual averaged cumulated snow, followed by the Indian Ocean sector (IOS) which brings 69 mm to annual averaged cumulated snow (Caiazzo et al., 2017).

Seasonally, four trajectories distribute equally except Western Pacific and Indian Ocean sector, which show maxima during autumn. Similarly, the seasonally averaged cumulated snowfall reaches the maximum values in summer and autumn for each sector, while WPO also showed a maximum in winter.

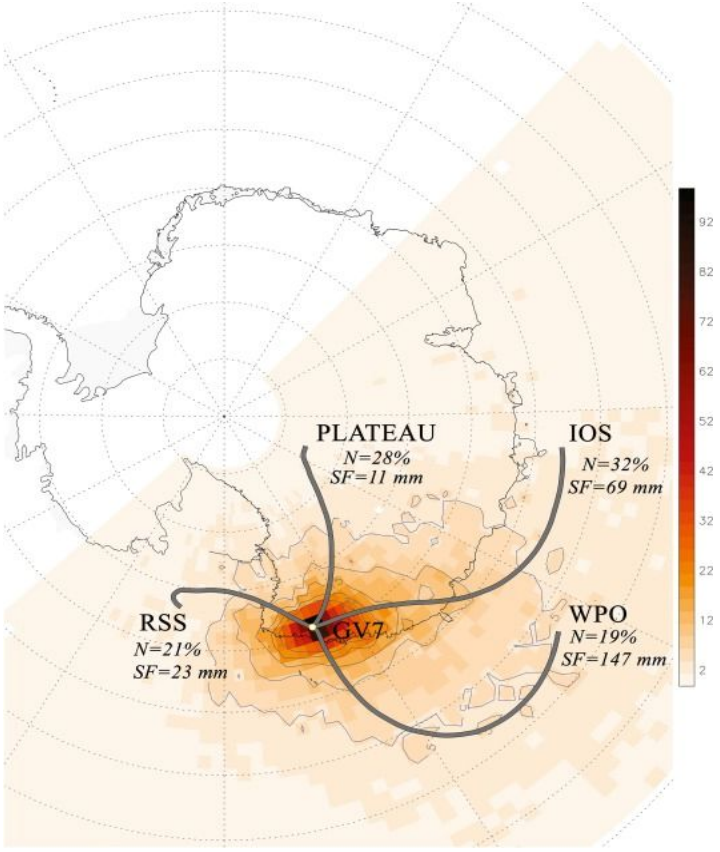

Fig 2.1.1 Representation of trajectories from four sectors (IOS, WPO, and PLATEAU & RSS) with the number of Trajectories (N) and annual average cumulated snowfall (SF) during 2007-2013 (Caiazzo et al., 2017).

The trajectories originating from the Western Pacific Ocean (WPO) bring 2 mm w.e./Tj due to few intense events in the Western Pacific, while trajectories from the Indian Ocean sector (IOS) and Ross Sea sector (RSS) are associated with 0.6 mm w.e/ Tj. The trajectories associated with the interior show a minor contribution to the GV7 site (Caiazzo et al., 2017).

2.2 Drilling Activity

Drilling activity was accomplished during the Antarctic field season 2013/14. In December 2013, a group of Italian and Korean scientists started drilling for deep and shallow ice cores at GV7. These ice cores were drilled 250 m south of the GV7 camp to avoid the influence of any human activity. During this operation, a snow pit of 384 cm was dug, with 127 3-cm samples collected along the three vertical parallel lines of the walls of the snow pit (Caiazzo et al., 2017). Besides, an intermediate ice core **(B)** of 250 m was retrieved, which could allow obtaining high resolution geochemical and paleoclimate records for the last 1-2 kyr. During the same campaign, a shallow ice core **(D)** of 12 m depth was retrieved 200 m south of the GV7 camp (Caiazzo et al., 2017), followed by even shorter firn core **(E)** of 5.7 m of depth, which allows observing recent changes in environmental conditions.

The annual average firn temperature at 10 m depth is -31.8 ° C (Frezzotti et al., 2007). Satellite studies of the slope, surface conditions, and wind direction suggested that the GV7 site is favorable for obtaining high-resolution records due to the low influence of katabatic winds and high signal-to-noise ratio (Magand et al., 2004; Frezzotti et al., 2007). GV7 site was examined through snow radar and GPS, showing horizontal and continuous internal layering in a 10-km boundary, which suggests that GV7 has a low ice velocity (0.30 ± 0.01 m yr^{-1}), as well as a spatially low snow accumulation variability (less than 5%) (Frezzotti et al., 2007). However, the use of at least 3-year average values has been suggested by those authors for obtaining a significant climatic signal from this site.

GV7 site is located on coastal Antarctica with an annual accumulation rate of 237 mm w.e for the last 150 years. A 55-m ice core was drilled at GV7 during the ITASE traverse, a mean snow accumulation rate of almost 241 mm/yr was determined at that occasion over the past 50 years (Magand et al., 2004; Frezzotti

et al., 2007). This accumulation rate was calculated using as an age marker the 1965-1966 radioactive horizon, associated with the 1963 nuclear bomb tests, revealed by a tritium activity identifiable peak (Stenni et al., 2002; Magand et al., 2004; Frezzotti et al., 2007).

3 Stable isotopic composition of snow

Water stable isotopes are considered efficient proxies for reconstructing past temperatures. Isotopes with characteristics of stability and non-radioactivity are known as "stable isotopes". In nature, water molecules have different masses depending on the number of neutrons characterizing oxygen and hydrogen atoms. Oxygen has three stable isotopes with different masses (^{16}O, ^{17}O, ^{18}O) while hydrogen has two different stable isotopes with a mass of 1 (H or ^{1}H) and mass of 2 (^{2}H or D), the latter commonly known as deuterium. ^{18}O and ^{2}H play a crucial role in understanding atmospheric and hydrological sciences (e.g. Gat, 1996). Different combinations of hydrogen and oxygen form nine water molecules, but in paleoclimate studies, three of these molecules ($^{1}H_2O^{16}$, $^{1}H_2O^{18}$ and $^{1}H^{2}H^{16}O$ or $HD^{16}O$) are of core importance. Out of these three molecules, $^{1}H_2O^{16}$ is abundantly available in nature while the rest of the two molecules comes under the category of rare water molecules.

Table 3.1- Water molecules with formulas and mean abundance in nature

Molecular Formula	**$H_2{}^{16}O$**	**$HD^{16}O$**	**$H_2{}^{18}O$**
Molecular Mass	18	19	20
Abundance	99.75 %	0.02 %	0.20 %

3.1 The δ-Scale

The δ-scale is used in stable isotope geochemistry for reporting isotopic measurements.

The isotopic content of a sample is quantified in delta per mil (δ‰), as introduced by Craig (1961a).

$$\delta\ ‰ = [(R_s - R_{std})/R_{std}] * 1000$$

Where δ ‰ is used for either $\delta^{18}O$ or δD, where R_s and R_{std} are the isotopic ratios of the sample and standard, respectively. The δ-unit is used to express the deviation of isotopic ratios (D/H, O^{18}/O^{16}) in a sample compared to the known isotopic ratios in a standard, which for water and oxygen in general is represented by VSMOW (Vienna Standard Mean Oceanic Water), set by the International Atomic Energy Agency (IAEA). The negative value of δ indicates an "isotopic depletion" and the positive value of δ are considered as "isotopic enrichment" of the rare isotope with respect to VSMOW.

3.2 δ-T Relationship

Paleo climatologists, for the last several decades, have found a linear relationship between mean annual stable isotope contents (δD and $\delta^{18}O$) of precipitation and local mean annual air temperature (Dansgaard, 1964; Jouzel et al., 1997).

The isotopic composition of Antarctic precipitation has been studied and analyzed in different parts of Antarctica including Vostok, Neumayer station, Dome F, and recently Dome C. The time series of these analyses, which span from 1 year to maximum one decade, suggested that there is a significant linear correlation between local temperature and isotopic composition of precipitation in Antarctica (Stenni et al., 2016).

However, the temperature correlation with the isotopic contents of precipitation is not always straightforward, therefore the spatial or temporal relationship of isotopic contents and site temperature must be regarded with caution. The parametrization of isotopic contents against local temperature can be highly affected by the rate of snow accumulation across Antarctica. Coastal Antarctica, with its high snow accumulation, offers a good correlation of spatial slope with season slope (Ommen and Morgan, 1997) and decadal slope, while other sites (Neumayer, Vostok, and Dome C) show a weak correlation, with a slope

for the $\delta^{18}O$-temperature relationship ranging from 0.35 to 0.65 ‰ $°C^{-1}$ (Casado et al., 2018). In order to understand the behavior of the δ-T relationship in the GV7 site, a preliminary survey was conducted by Becagli et al. (2004).

3.3 The Global Meteoric Water Line (GMWL)

Harmon Craig (1961), published in his findings that $\delta^{2}H$ and $\delta^{18}O$ correlate on a global scale in freshwater. Craig defined the "Global Meteoric Water Line (GMWL)" with the following equation:

$$\delta^{2}H = 8\ \delta^{18}O + 10\ ‰\ SMOW\ (Craig, 1961)$$

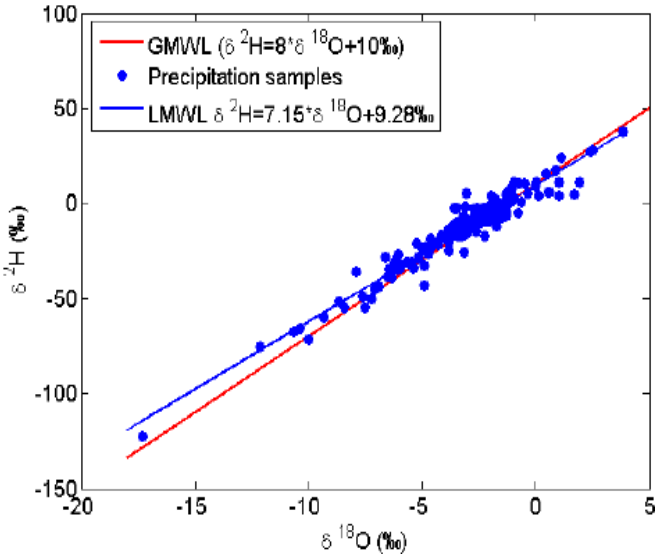

Fig.3.3.1- The Global Meteoric Water Line (GMWL) for precipitation worldwide. Source: Rozanski et al. (1993)

This equation proved that the composition of meteoric waters behaves in predictable fashion such that $\delta^{2}H$ and $\delta^{18}O$ are linearly related with a slope of 8 and thus defined the so-called GMWL (Craig, 1961) which shows high values in the tropics and low values near the poles.

3.4 Deuterium excess: A moisture source proxy

In equilibrium conditions, δD is linearly related to $\delta^{18}O$, but studies have found that in a kinetic fractionation, water stable isotopes show slightly different behavior (Dansgaard, 1964). Therefore, to quantify this slight deviation from the norm, the second-order parameter "deuterium excess" (d) is used,

expressed by the following equation

$$d = \delta D - 8*\delta^{18}O \ (‰)$$

derived from the Global Meteoric Water Line (Craig., 1961): $\delta D = 8*\delta^{18}O+10$, where 10 represents the deuterium excess in average global precipitation.

According to Dansgaard (1964), d-excess is determined in water vapor formation at the moisture source and remains constant in Rayleigh rainout (Gat, 1996). Deuterium excess is mainly dependent on the climatic conditions (sea surface temperature, relative humidity, and wind speed) at the moisture source region of precipitation (Merlivat and Jouzel, 1979). Stenni et al. (2001), investigated the relationship between d-excess and those parameters and interpreted the d-excess variability for the EPICA Dome C ice core as mainly dependent by sea surface temperature (SST) with low impact of relative humidity. However, Stenni et al. (quaternary science review, 2010), suggested that the d-excess must be considered an integrated proxy of the hydrological cycle rather than SST variability at a fixed position in the ocean. Steffensen et al. (2008), studied the d-excess record from the NGRIP Greenland ice core and found fast (1-3 yr.) changes in d-excess related to fast changes in the atmospheric circulation associated with conditions at moisture sources.

However, the extremely low condensation temperature of the snow in inland Antarctica also affects d-excess values (Stenni et al., 2001). The main drivers of d-excess still could not be exactly figured out by scientists, but recent studies suggest that relative humidity of moisture source mainly influences the d-excess values (Pfahl and Sodemann, 2014).

3.5 Post depositional effects

Since the advancement in infrared laser spectroscopy, which can provide the rapid measurement of isotopic contents of snow and vapors, there have been different advancements in understanding the processes which affect the signal of isotopic contents of surface snow. In order to study the difference of slopes between seasonal cycle of isotopic composition and temperature (Ekaykin et al., 2004; Stenni et al., 2016) and

spatial slope of isotopic composition and temperature (Masson-Delmotte et al., 2008), the local isotopic exchange between vapor and snow has been recently addressed (e.g Casado et al., 2018). According to these findings, the slope of surface snow isotopic contents were found different than the one found in precipitation, which is possibly affected by cumulative effect of intermittency in precipitation (Genthon et al., 2015), patchiness of accumulation, an exchange of water molecules between local atmosphere and snow (Casado et al., 2016b), wind across the site resulting in an irregular redistribution of freshly fallen snow (e.g.,Ekaykin et al., 1998) and exchanges within firn affecting the isotopic signals. Additionally, the temperature gradient in the snowpack can result in sublimation, molecular diffusion, and condensation, which can influence isotopic signals of firn (Gkinis et al., 2014). Since the strength of post-depositional processes is inversely related to the snow accumulation rate, sites with a high accumulation rate such as GV7, are characterized by a well-preserved isotopic signal and could show a good δ-T relationship.

4 Reanalysis and Model Data

4.1 ERA-Interim Model

Climate reanalysis provides key information to validate the proxy records from ice cores in those parts where direct observations are difficult to make due to a lack of meteorological stations. Although proxy records have been calibrated with reanalysis data for the more recent period, it should also be considered, that reanalysis data are not exempt from biases and uncertainties.

The ERA reanalysis, from the European Center for Medium-Range Weather Forecasts (ECMWF), is the data assimilation system that advances forward in time on cycles where the available observation in combination with forecasts to extract the evolving state of atmosphere and surface beneath. ERA-Interim was generated to replace ECMWF re-analysis (ERA-40) and introduce a generation of Global Atmospheric Model (GCM) with the advancement in the hydrological cycle and stratospheric circulation pattern. Additionally, the four-dimension variation (4DVar) analysis system has been utilized for temporal consistency, correcting and improving humidity analysis and handling.

Since 1979, ERA-Interim data is available at 0.7-degree resolution (~70km) with six hours interval. As mentioned earlier, reanalysis data are not exempt from uncertainties.

4.2 ECHAM5-wiso Model

The climatic interpretation of stable isotopes in Antarctic precipitation is a challenging task. In order to retrieve information from these climate archives, quantitative approaches have relied on these empirical relationships. For producing reliable information, state-of-the-art General Circulation Model (GCM) has become a key to quantitatively explore the Spatio-temporal relationship between precipitation isotopic composition and temperature. The ECHAM5-wiso model used in this study is nudged to ERA-Interim global atmospheric reanalysis. The data used in this thesis, which covers the period 1979-2012 at a daily resolution, have been provided by Martin Werner from the Alfred Wegener Institute (AWI) in Germany. In order to compare isotopic data with model data, we have extracted 2-m surface air site temperature for

the 1979-2012 period from ERA-Interim which was then averaged into annual values.

ECHAM5-wiso is equipped with precipitation stable water isotopes (Werner et al., 2011b), which has been utilized for realistic simulation for observations of isotopic composition in precipitation and water vapor on a global scale. Earlier it was documented that the simulated mean annual isotopic composition by ECHAM5-wiso, is in good agreement with the spatial isotopic dataset compiled from snow and ice-core data (Goursaud et al., 2017). In comparison with ECHAM3, the hydrological cycle of the ECHAM5-wiso model has been equipped with the main stables water molecules ($H_2{}^{16}O$, $H_2{}^{18}O$, and HDO) in a more analogous way (Goursaud et al., 2017). Additionally, the ECHAM5-wiso model is implemented individually with each water phase (vapor, cloud liquid, cloud ice) along with its isotopic counterparts in the model code. Since isotopic fractionations are key to carry out a quantitative approach for isotopic contents, the ECHAM5 model was implemented with equilibrium and kinetic fractionation during each water phase.

In our study, we use the ECHAM5-wiso model for isotopic contents ($\delta^{18}O$, δD), precipitation and temperature, while ERA-Interim reanalysis data for precipitation and 2-m air temperature; all of these are used for comparing with isotopic data from ice cores.

We used the ECHAM5-wiso model data comparison to address the key questions: **(i)** is there any correlation of ECHAM5-wiso model data with the ice core data on an inter-annual scale, trends or remarkable years? **(ii)** How significant relationship exists in the isotopic contents from ice cores and simulated 2-m air temperature and what could be the possible reasons for any discrepancies?

The datasets from ice cores include snow accumulation on annual bases, isotopic contents, and calculated d-excess, while datasets from ERA-Interim and ECHAM5-wiso models include precipitation, temperature and isotopic contents of precipitation.

4.3 El Niño–Southern Oscillation (ENSO)

El Niño is a complex series of climatic changes in the equatorial pacific resulting in usually warm water bringing droughts in Australia and unseasonal heavy rains in South America. El Niño is considered a major source of variabilities in global precipitation on 2-8 years of time scale (Rahaman et al., 2019). However, the recent studies suggested, that these changes could be the result of the coupling of ENSO and Pacific Decadal Oscillation (PDO) and may have an effect on Antarctica due to southern hemisphere teleconnection, which has been found throughout Antarctica in observational and reanalysis data (Welhouse., 2016).

Previous findings regarding the ENSO effects in Southern Hemisphere suggested that Western Antarctica is consistently found with ENSO signal in ice core records. Further, proxy records from Eastern Antarctica have shown an increasing trend in Temperature in ENSO bands (Welhouse, 2016). Similarly, proxy records from ITASE 01-5, showed a prominent pattern found in agreement with reanalysis data and suggested, that the high accumulation may align with the seasonality of ENSO signal in this region.

For this thesis, we used the Niño 3.4 SST index, calculated from the HadISST1; It is the area-averaged SST from 5S-5N and 170-120W (NOAA, 2019).

It is possible to see the sub-annual signals in ice core records from high accumulation sites (Turner, 2003). Since GV7 has a high annual snow accumulation rate, we will use proxy records and reanalysis data of isotopic contents, accumulation, and temperature on a shorter timescale (1979-2012) to investigate: **(i)** is there any impact of ENSO in isotopic records from GV7? **(ii)** The slope between proxy records and ENSO. **(iii)** If there are any remarkable inter-annual variations in proxy records during strong ENSO years since 1979 and whether the reanalysis data agrees with these fluctuations.

4.4. Southern Annular Mode (SAM)

The Southern Annular Mode (SAM), which is also known as the Antarctic Oscillation (AAO), is the low-frequency mode of atmospheric variability where the north-south movement of westerly wind encircles Antarctica and brings cold and warm periods based on its positive and negative phases. It was documented

that SAM has a strong influence on the temperature variabilities in Antarctica (Marshall et al., 2013). The cold anomalies in coastal East Antarctic since the 1990s interpreted as a trend to be linked with the positive phase of the SAM (Marshall, 2007). However, satellite data revealed that it was also the case across West Antarctica. Moreover, Marshall (2006), stated that the SAM-Temperature relationship remained consistent across all four seasons.

Furthermore, the cooling effect by the combination of positive-negative trends was described as "shielding" in East Antarctica from "global warming" (Marshall et al., 2013). In agreement with this statement, Marshall (2006) found out that SAM-positive based cooling exceeds 1°C in autumn in most of the East Antarctica stations. Based on these assumptions and findings, we have taken the SAM dataset spanning from 1979 to 2012 to quantify the interannual impacts of positive and negative SAM phases on the temperature, isotopic contents, and accumulation at GV7 which is situated in eastern coastal Antarctica.

For this thesis, we used the Antarctic Oscillation Index from the National Oceanic and Atmospheric Administration-NOAA (2019), defined by surface atmospheric pressure patterns.

4.5. Sea Ice Extent (SIE)

Sea ice extent controls a larger part of temperature and moisture availability (Sime et al., 2019). GV7, as mentioned earlier, receives moisture from four different sectors which were reconstructed through a backward trajectory model. Therefore, in this study, we focus on the sea ice extent influence the variability of deuterium excess to understand the source of moisture in this region. We have used the data of sea ice extent of the Western Pacific Ocean, Ross Sea, and the Indian Ocean, which are the three major contributors for GV7 precipitation. Further, we will take ECHAM5-wiso model data for d-excess, which could be linked to the sea ice extent, to compare our results from ice cores. For this research study, the data of sea ice extent was taken from National Snow and Ice Data Center (NSIDC) available at http://nsidc.colorado.edu/data/ .

5 Material and Methods

The ice core chemical and isotopic analysis were carried out in Italy and South Korea for the Korean core. The isotopic ($\delta^{18}O$, $\delta^{2}H$, d) measurements were performed at the geochemistry laboratory of the Ca' Foscari University of Venice, Italy. Samples were preserved in sealed-air-tight bags at -20 °C. In order to avoid any alteration of the isotopic composition of these samples by air contact, they were transferred to HDPE (High-Density Polyethylene) 25-ml Kartell bottles until their measurement. 8,000 samples were obtained from the cutting of all the ice cores at GV7. Bag samples are low-resolution samples of 60 cm, while high-resolution samples consist of 4 cm samples. The initial samples taken from core B started at a depth of 3 m and were measured until ~16m of depth. While core D and E samples were measured for its entire length of 12 m and 5.7 m respectively. For this thesis work I contributed with the analysis of almost 350 samples, the other isotopic data, produced by the geochemistry laboratory group, have been made available for this thesis in order to cover the period 1979-2012.

The isotopic measurements were performed with a Thermo-Fisher Delta Plus Advantage Isotopic Ratio Mass Spectrometer (IRMS), coupled with an automatic equilibration device (HDO) and with a Picarro L1102-*i* Cavity Ring-Down Spectroscope. All the measurements are reported against VSMOW. Analytical precision of these measurements is ±0.05‰ for $\delta^{18}O$, ±0.7‰ for $\delta^{2}H$, with a final precision on the calculated deuterium excess of ±0.8‰ for the IRMS measurements, while the precision of the Picarro measurements is ±0.1‰ and ±0.5‰ for $\delta^{18}O$ and δD, respectively.

5.1 Mass Spectrometer

The Isotopic Ratio Mass Spectrometry (IRMS) technique is used to calculate the relative deviation of the isotopic ratio (in our case $^{18}O/^{16}O$ and D/H) in a gas sample relative to the same ratio in standard gas. The IRMS (Fig 5.2.1.1), components show an inlet jet for handling the pure gas and avoiding isotopic fractionation, contamination or memory in electron ionization source (IE). There is an analyzer system for detecting simultaneous ion currents. This analyzer system consists of a flight tube, collector and faraday cups along an image plane. This whole unit is systematically synchronized with a computer-controlled data

acquisition system.

Samples are introduced into a 5-ml glass vial together with internal water standards calibrated against VSMOW and SLAP. There are 24 glass vials attached to the equilibration unit. The water samples are then equilibrated with ultra-pure gasses (H^2 for δD and CO_2 for $\delta^{18}O$), following the below reactions to the equilibrium state.

$$H_2{}^{18}O + C^{16}O_2 \longrightarrow H_2{}^{16}O + C^{16}O^{18}O \text{ for } CO_2$$

$$HDO + H_2 \longrightarrow HD + H_2O \text{ for } H_2$$

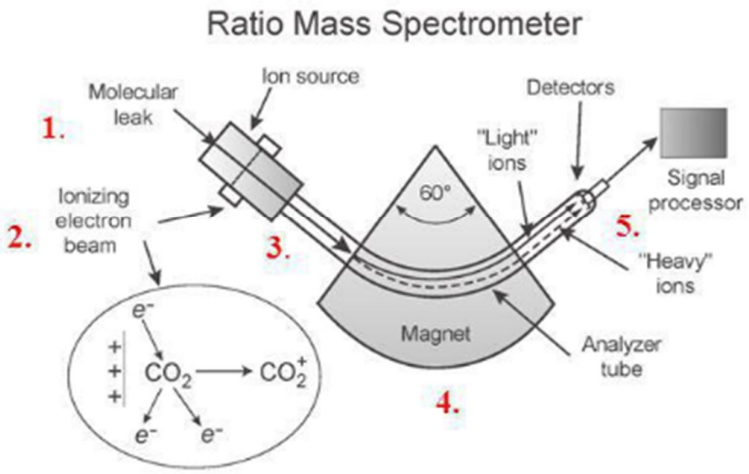

Fig. 5.1.1- Isotopic Ratio Mass Spectrometer (IRMS) components.

The equilibration times for H_2 (in presence of a platinum catalyst) and CO_2 are 2 and 10 hours, respectively. During this process, a thermostat bath keeps shaking at 18℃. The pumping system generates a high vacuum inside the analyzer system which causes the residual gas molecules to drop down to less than 1% compared to molecules introduce for analysis. The dual-inlet is a high precision technique as compared to the continuous flow system. Separate variable volume keeps the adjusted pressure of both reference and sample gases and introduces them into the ion source as soon the identical amount of reference and sample gas is

generated. After the equilibration of gas with water sample (or water standard), it is injected into the ion source of the mass spectrometer, where an electron beam from a white-hot tungsten filament, ionizes the gas.

The ions are further accelerated and focused by a magnetic field, where they are deflected towards a circular path. Since the curvature radius depends on the charge-to-mass ratio, therefore ions are separated on the charge-to-mass ratio and later the strength of the magnetic field and accelerated voltage defines the trajectory of these ions. The surface of Faraday cups emits an electron for every trapped ion and these ions are amplified and detected as a current. Thus, the relative abundance of isotopes from molecular species can be measured through a current associated with a specific isotopologue. Finally, the computer linked to the mass spectrometer processes the results and produces the output as a ratio compared to the reference standards, in terms of isotopic composition and δ values.

The CO_2/H_2 water equilibrium unit is coupled with a dual-inlet (Fig.5.2.1.2) mass spectrometer.

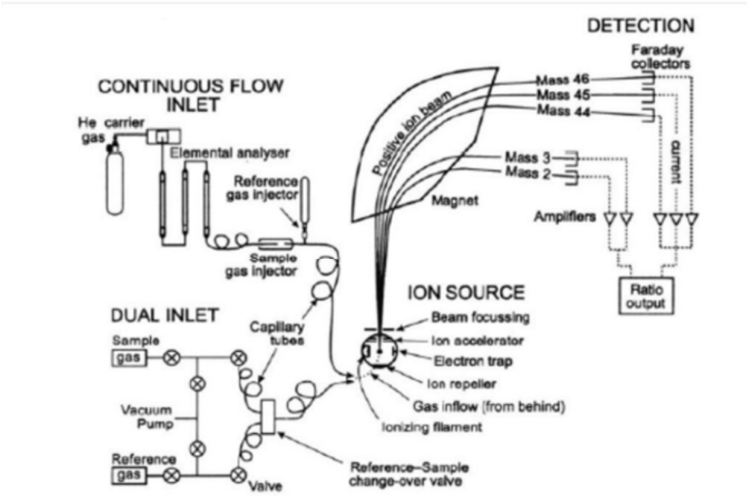

Fig 5.1.2- Diagrammatic representation of isotope ratio mass spectrometer (IRMS) with dual-inlet and continuous flow. Source: www.gwadi.org

5.2 Cavity Ring-Down Spectroscopy (CRDS)

Cavity ring-down spectroscopy (CRDS) is capable of measuring a small amount of water (down to 300 µl). Although the Picarro L1102-*i* laser spectroscope used for this study is not as precise as an IRMS, it

takes less time for sample measurement. CRDS (Fig 5.2.2.1) uses a laser absorption technique for the quantitative detection of molecular species with high sensitivity. CRDS uses an infrared laser for direct detection of different isotopologues, thus enabling direct measurement of $\delta^{18}O$ and δD. A laser pulse is emitted through a high-finesse optical cavity containing the sample, where the laser beam bounces back and forth on the highly reflecting mirrors, covering a path of 12 km; the pulse decay is then monitored with the aid of a detector that measures the intensity of the light transmitted through one of the mirrors. This absorption technique is based on the Lambert-Beer law equation, meaning the light intensity decreasing through a medium is associated to the interaction with the medium: $I = I_0^{-\alpha x}$ where I_0 and I are the light intensities before and after crossing the medium, α is the absorption coefficient and x is the path length. The absorption rate depends on the sample concentration and on the optical path length.

CRDS is based on the different absorption peaks in the near-infrared of each water isotopologue, which shows their vibrational mode given by the masses of their atoms. In this technique, the absorption time is calculated before and after the sample is injected and the difference between the two times is used to calculate the concentration of the absorbing species (Fig.5.2.1).

As already mentioned, a Picarro L1102-*i* liquid water analyzer was used for this study, where the water samples are introduced in a vaporization chamber which vaporizes the water at a temperature set at 110°C.

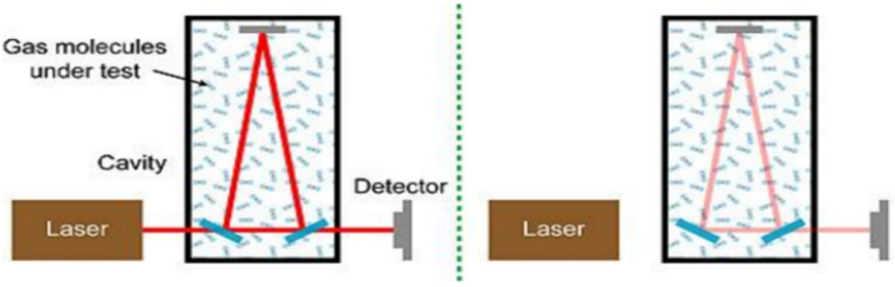

Fig 5.2.1- The basic principle of Picarro CRDS involving the laser impulse that is trapped in a three-mirror cavity. Source: www.articles.sae.org

Once the vaporized sample reaches the cavity, a short laser pulse with a specific near-infrared wavelength is emitted by a diode. After reaching a threshold, the laser is turned off and the light bounces back and forth in the cavity using three high reflecting mirrors. The photodetector, placed behind one of the mirrors, measures the exponential decay of the beam.

In order to minimize the memory effect produced by the previous sample, each sample is analyzed eight times (eight consecutive injections). Each datum passes through an outlier test and the average value of the remaining repetitions is computed for each sample; each repetition falling off the $\pm 1\sigma$ interval is discarded, while the average of the remaining values is calibrated using a line given by "true" and measured values of internal standards used in this analysis.

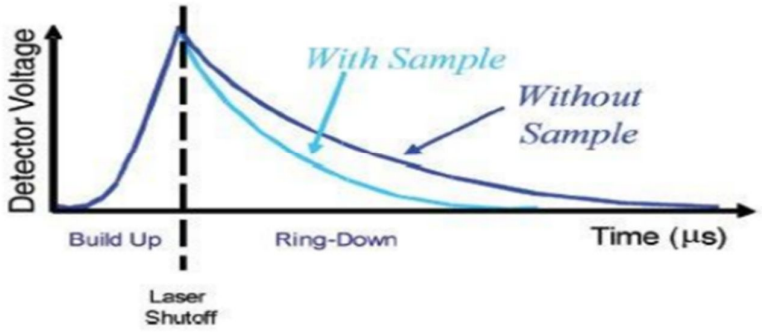

Fig 5.2.2- Light intensity as a function of time in a CRDS system with and without a sample having resonant absorbance. Source: www.americanlaboratory.com

5.3 Statistical Analysis

Statistical Analysis of proxy and reanalysis data were carried out by the R environment for statistical computing and visualization. This analysis was used for finding correlations of variables from observation data and model data (ECHAM5 & ERA-Interim), as well as correlation and significance level in the proxy data such as the correlation significance of δ and T relationship, accumulation (GV7) to precipitation (model), d-excess to isotopic contents, sea ice extent to d-excess, El Nino-to-isotopic contents and so on. Since the proxy data span on a short timescale, no data cleaning was required as well as the data distribution remained normal. Some of the statistical computations below were performed for this research study.

5.3.1 Data Visualization

Data visualization technique is used to find out the visual data distribution through a specific time period (in our case 1979-2012). We used some visualization tools such as "ggplot2" (95 % confidence interval) and "plotly" to see the variabilities of isotopic contents through different years and finding out any remarkable change. We use a "plotly" package on the R environment to compare the pattern and phasing of more variables ($\delta^{18}O$, d-excess, accumulation) over the same time period. Moreover, we also utilized MATLAB (version- R2018b) visualization techniques for a detailed examination of the signals of different variables such as SAM, $\delta^{18}O$, and accumulation.

5.3.2 Linear Regression

In order to calculate the correlation coefficient and significance level between different variables included in our data (e.g $\delta^{18}O$ and temperature, d-excess and sea ice extent, precipitation and accumulation etc.), we used a simple linear regression tool in R. This tool was used to compute the influence of independent variable (e.g. temperature, ENSO, accumulation, etc.) on the isotopic contents. For this, we use the "lm () function "Linear Model" with different arguments (fitting linear model).

$$Y = \beta_o + \beta_1 A$$

Where βo is the theoretical y-intercept and β1 is the theoretical slope in this formula. R is equipped to provide four various graphical approaches to evaluate the model and the suitability of data for Linear regression. Further, to obtain statistical information of a model, we use "summary () function which provides us with a significance level (*p*-value) and correlation (R-squared) along with standard deviation ("std dev") and "t-statistics".

6 Results

6.1 Isotopic Data against Depth

In order to understand the spatial variability of isotopic composition and local and regional climatic conditions at GV7, 3 ice cores (B, D, E), with different temporal extensions were collected within ~10 m distance from each other (Table 6.1.1). Additionally, to avoid any stratigraphic noises, we took the stacked record of all the ice cores plus the ITASE core collected during the 2001-02 traverse (Genoni, 2008) to provide a robust analysis of this part of Antarctica.

Table.6.1.1- The ice cores from GV7 with depth (m) and period covered.

Core	Depth (m)	Period
B	3-16.1	2007-1979
D	0-12	2012-1990
E	5.7	2012-2003

In this section, we present the stable isotopes data (δD, $\delta^{18}O$, and d-excess), against depth (m) from 3 ice cores (B, D, E).

The ice core data considered and analyzed for this study covered the last 34 years (1979-2012). The second-order parameter, deuterium excess was calculated ($d=\delta D - 8*\delta^{18}O$) from the co-isotopic analyses of δD and $\delta^{18}O$. In table 6.1.2, we report the isotopic data with their maximum, minimum and average values including the standard deviation for each core.

Parameter	*Core B*	*Core D*	*Core E*
δ^{18}O (‰)			
Min	-37.14	-38.05	-38.07
Max	-22.94	-23.27	-25.15
S.dev	2.69	2.45	2.34
Mean	-29.64	-30.4	-30.09
δD (‰)			
Min	-295.11	-302.72	-303.73
Max	-171.92	-177.01	-173.06
S.dev	22.59	20.93	21.35
Mean	-233.12	-235.06	-234.11
d-excess			
Min	-1.62	-0.96	-0.55
Max	11.63	12.39	11.18
S.dev	2.15	2.48	2.61
Mean	3.99	5.14	4.76

Table 6.1.2- Isotopic composition min, max and average values (plus the standard deviation) from each ice core.

6.1.2 Core B

The δD, δ^{18}O and d-excess profile for core B are reported against depth in meters (Fig 6.1.2). As expected, we observed (Fig 6.1.2) a striking similarity in δD and δ^{18}O records. The average values for δD and δ^{18}O were -233.12 ‰ and -29.64 ‰, respectively. A clear seasonal signal is observed along with the record, with less negative values during summer and more negative values during winter. Moreover, we noticed that there is a decreasing trend in the isotopic contents from 5-10 m and 11-14 m depth. The depth profile of d-excess calculated from δD, δ^{18}O, showed in phase agreement with the δD, δ^{18}O. However, the depth profile of δD, δ^{18}O and d-excess in core B, shows a downward shift after ~6 m depth in the isotopic contents.

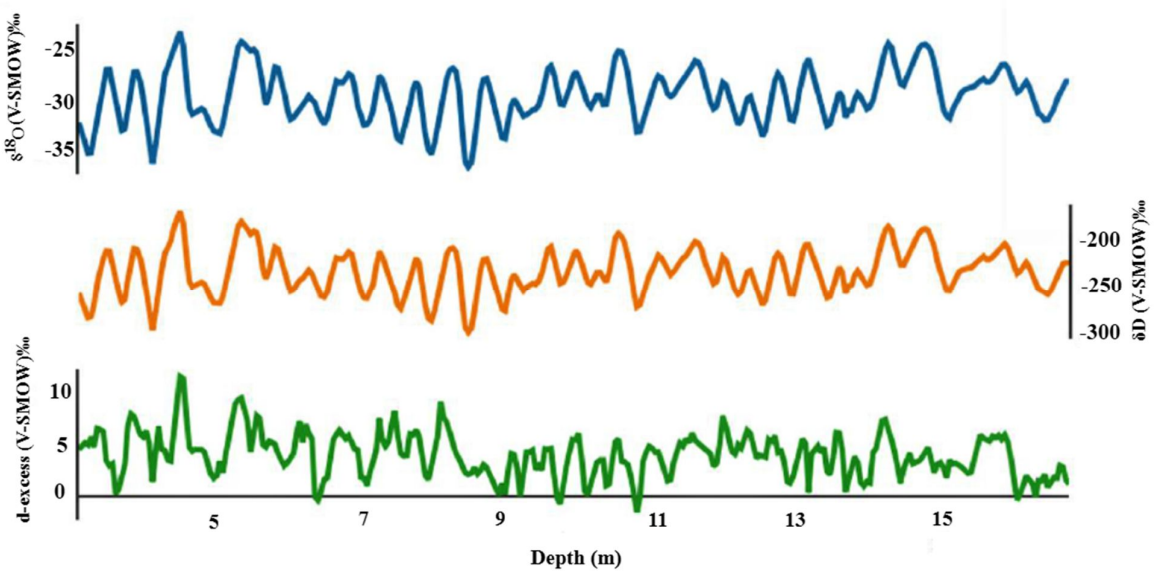

Fig.6.1.2- Snow depth profiles of $\delta^{18}O$, δD and d-excess in core B

6.1.3 Core D

Core D with a length of ~12 m (Fig.6.1.3), spans from 2012 to1990 (1989 and 2013 were discarded due to incomplete data), which additionally covered (0-3 m), the isotopic composition from the surface which had not been previously covered by core B.

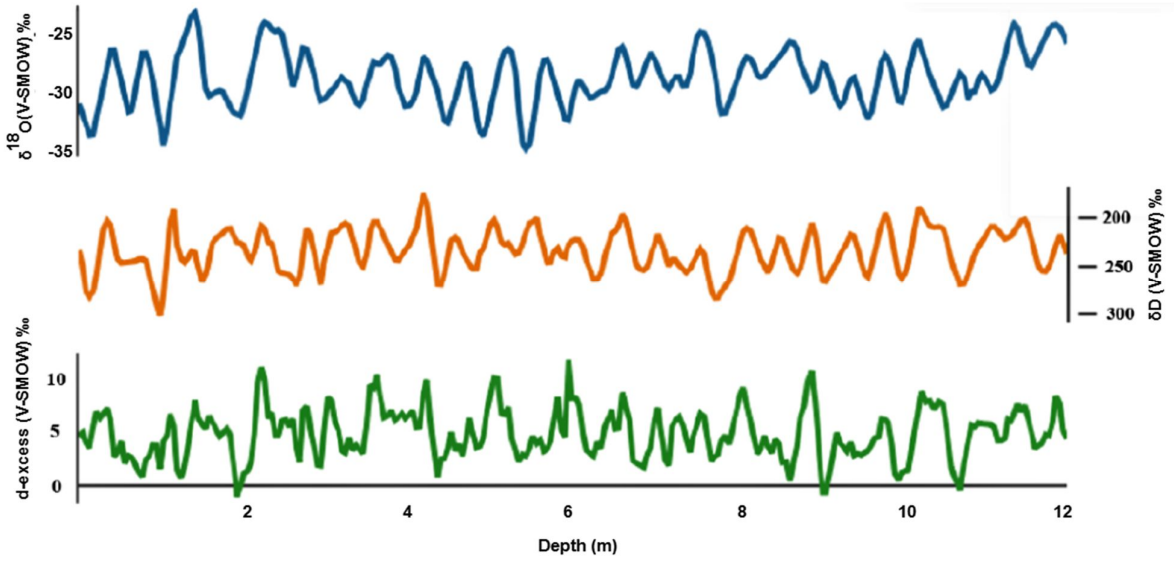

Fig. 6.1.3- Snow depth profile of core D

Although the isotopic values for δD, $\delta^{18}O$ almost remained the same (average -234.06 ‰ and -30.04 ‰) as in core B, the deuterium excess showed an average higher value (5.14 ‰). Also, in this case, a clear seasonal signal is visible.

6.1.4. Core E

Core E is a shallow firn core with a depth of 5 .7 m (Fig 6.1.4), covering the period from 2013-2002. Due to incomplete data of isotopic contents in 2013 (drilling year) and 2002 (end-depth), we limited the measurement from 2012-2003. The measurement of isotopic contents in core E did not show any prominent deviation from the isotopic values of core B and D. Additionally, the average isotopic values for δD, $\delta^{18}O$ and d-excess were found as -234.11 ‰, -30.09 ‰ and 4.76 ‰ respectively. Again, the seasonal variability is evident.

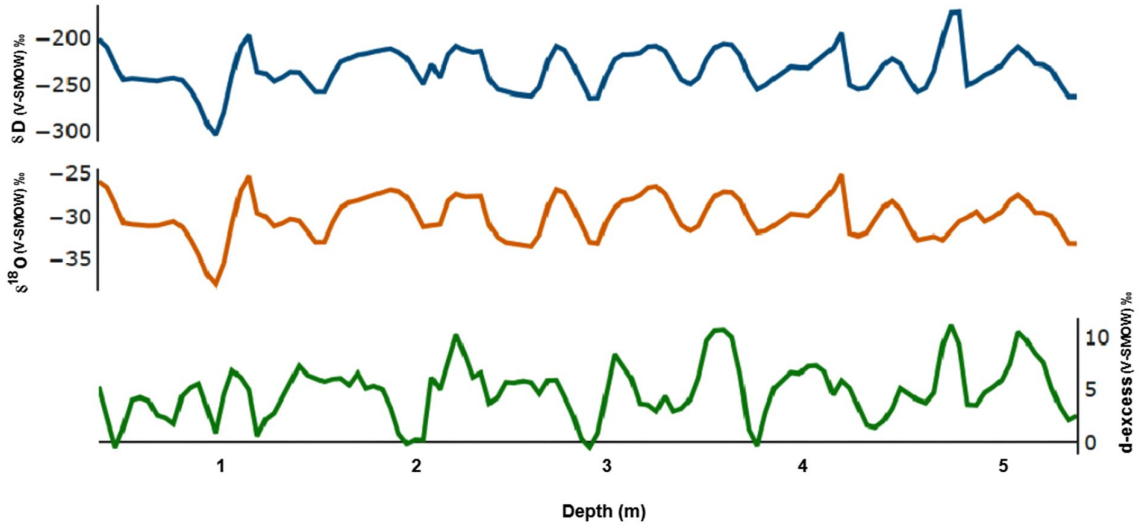

Fig. 6.1.4- Snow depth (m) profile of core E.

6.1.5 Stable isotopes against Global Meteoric Water Line

The slope and intercept of covariance between the water stable isotopes (δD & $\delta^{18}O$), defined by Craig (1961) and called GMWL, is 8 and 10, respectively.

Since we have 3 ice cores, we have constructed separate Local Meteoric Water Lines (LMWL) at a different scale i:e raw, annual and 3 years moving average.

In core B and D (raw), we found that the slope is 8.33 and 8.47, respectively, in agreement with the slope of GMWL (i.e. 8).

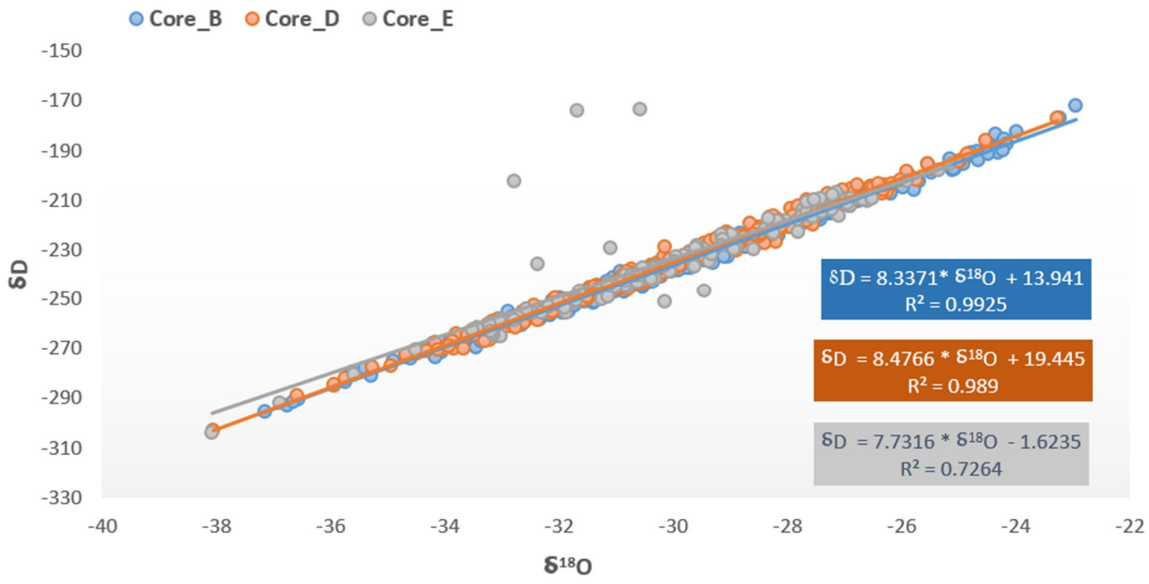

Fig. 6.1.5a- LMWL for core B, D, and E using $\delta^{18}O$ and δD raw data.

Additionally, the ($r^2 = 0.99$), showed a strong correlation between δD & $\delta^{18}O$ for core B and D. However, core E (raw), depicts a small decrease in the slope (7.73), followed by a drastic decrease in the intercept (1.62 ‰), including a strong yet a weaker correlation ($r^2 = 0.72$) between δD & $\delta^{18}O$ as compared with core B and D.

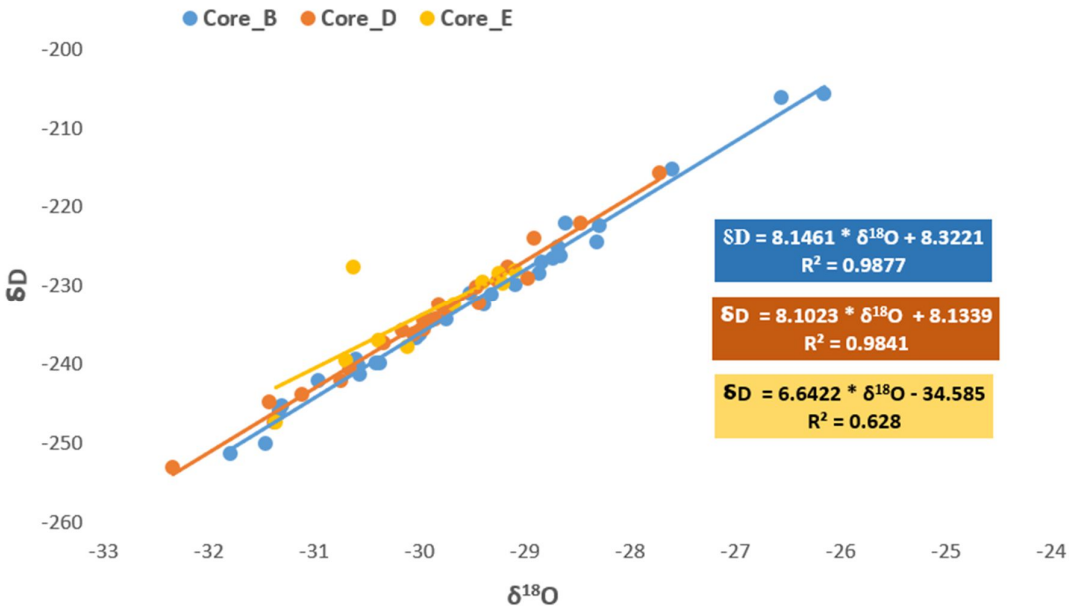

Fig.6.1.5b- Core B, D and E LWML on the annual timescale.

In order to minimize the non-climatic noises and false fluctuations in the data, we constructed LMWL for the 3 cores on annual basis (Fig. 6.1.5b), which suggested, that the slope (8.14 and 8.10) for core B and D respectively, are in agreement with GMWL, while a slight decrease of 1.68 ‰ and 1.87 ‰ (respectively) recorded in the intercept. Moreover, core E shows a prominent decrease in the slope (6.64) against GMWL (i.e. 8) and -34.58 ‰ in the intercept, with a correlation of (r^2= 0.62) between δD & $\delta^{18}O$.

The three years moving mean of isotopic contents were used to construct a further LMWL (Fig. 6.1.5c), where core B, showed a surprising decrease in the intercept (3.27 ‰), while core D with 18.03 ‰ showed an increase of 8‰ against GMWL (10‰).

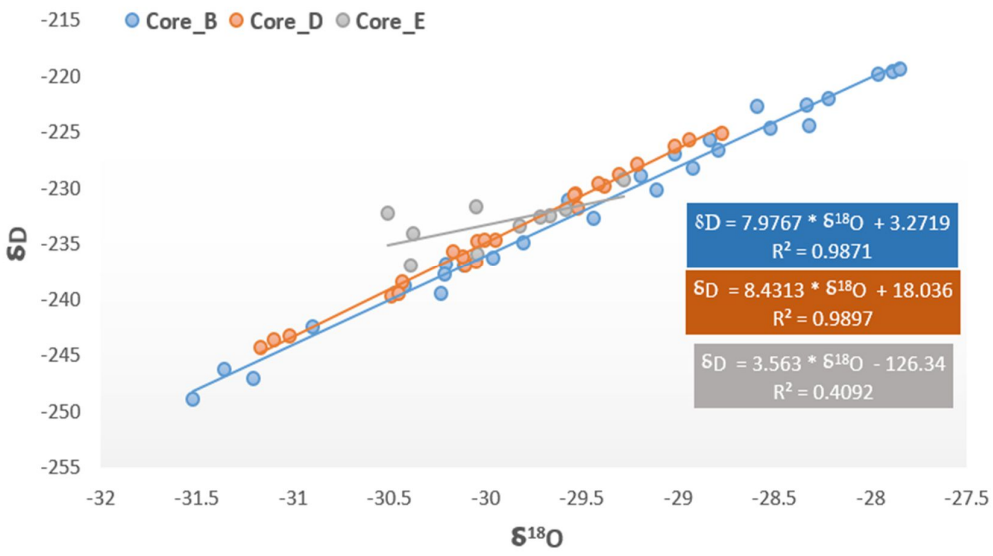

Fig.6.1.5c. LMWL of 3 years moving average for core B, D, E**.**

The slope in core B and D (7.97 and 8.43) respectively stayed close to the slope of GMWL (i.e. 8). Furthermore, core, E, showed a huge decrease in the slope (3.56 ‰), along with the intercept of -126.34 ‰. The high dissimilarities of core E in slope and intercept values can possibly suggest the post-depositional process, which could modify the isotopic composition. These variations in d-excess against GMWL will be discussed later in the discussion section.

6.2. Dating of ice cores

Studying ice cores for the reconstruction of past climatic conditions needs a reliable and validated age-depth scale. There have been various approaches to generate a consistent chronology. The detection of annual layers of stable isotopes (δD & $\delta^{18}O$) has been preferred for obtaining high-precision chronology of ice cores, which we applied in this research study (Fig. 6.2.1). Since δD & $\delta^{18}O$ have striking similarities in their distribution along with the depth, we choose to observe the seasonal minima and maxima of $\delta^{18}O$ for creating the chronology for all the 3 cores.

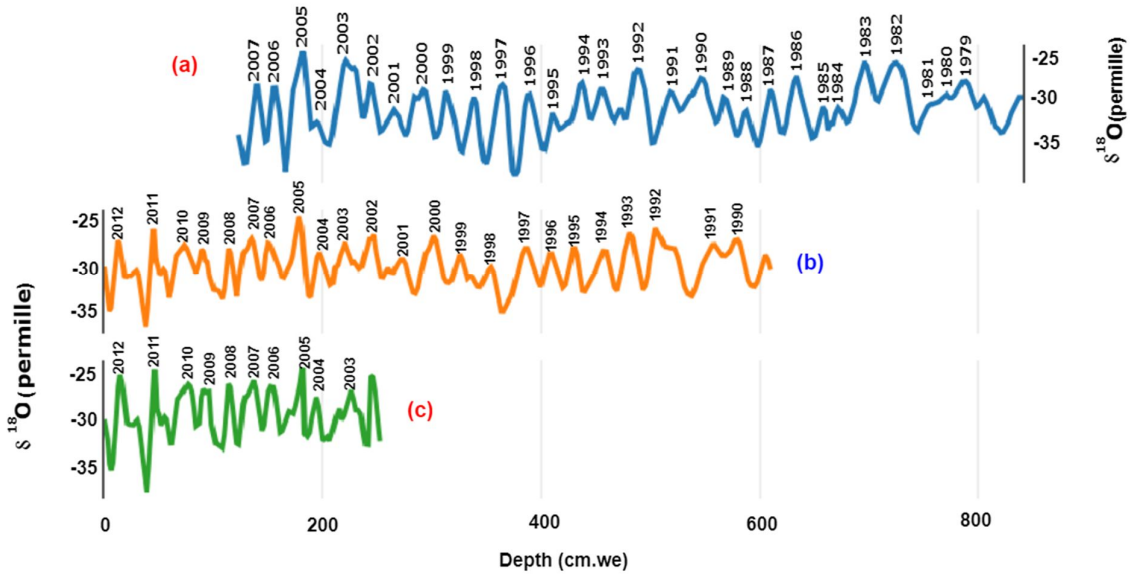

Fig.6.2.1- ice cores dating using the austral summer peaks of $\delta^{18}O$. **(a)** core B **(b),** core D **(c)** and core E.

The $\delta^{18}O$ signals for summer (maxima) and winter (minima) are connected to local or regional temperatures and result in obtaining reliable information on the seasonal cycle of temperature at the site.

However, to obtain visible $\delta^{18}O$ summer (austral) maxima, the thickness of layers is of utmost importance. The thickness of the annual layers depends on the amount of annual accumulation. Since GV7 is a coastal site with a relatively high annual accumulation, we identified the prominent $\delta^{18}O$ summer maxima for creating a chronology for all cores. Although $\delta^{18}O$ signals can be distorted along with depth through diffusion, our records since 1979 for isotopic signals remained preserved due to high accumulation rate and no considerable post-depositional processes at the site.

For obtaining a robust chronology of $\delta^{18}O$ along with depth, we performed a comparison with $nssSO_4$ profile (Fig. 6.2.2), produced at the University of Florence and courtesy made available for this thesis.

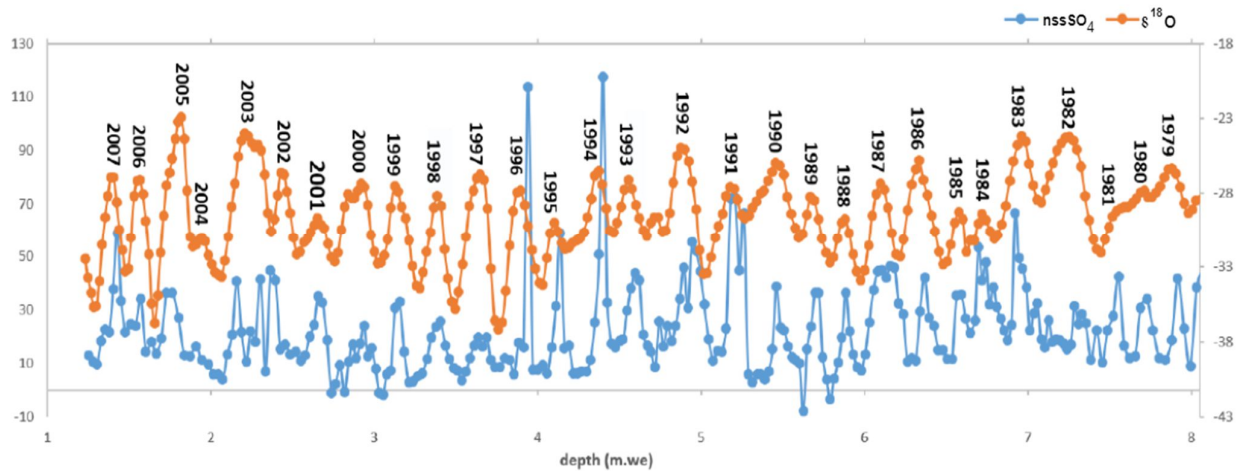

Fig.6.2.2- $nssSO_4$ in comparison with $\delta^{18}O$ from core B (performed for all cores). $nssSO_4$ shows summer maxima which agrees with the $\delta^{18}O$ peaks of austral summer.

$nssSO_4$ is constituted of several components i.e. compounds produced by phytoplankton, volcanic constituents and other extra polar sources from the upper and lower troposphere (Caiazzo et al., 2017). The biogenic and non-biogenic sources in $nssSO_4$ tend to show a peak in the early summer due to phytoplanktonic blooms and breakdown of the polar vortex, respectively. Moreover, $nssSO_4$ is a useful proxy in indicating the volcanic events. Well-dated volcanic events can be used as reference markers by observing remarkable spikes in the $nssSO_4$. However, isotopic dating of shallow firn cores (core E in our case), has no reference date of volcanic events, yet we used the early summer peaks in $nssSO_4$ as a comparison.

6.3. Annual isotopic temporal series

To determine inter-annual isotopic temporal distribution and accumulation, we utilized the stable-isotope well-preserved signals from the depth profile of each core.

We took the mean annual values of δD, $\delta^{18}O$ and d-excess, whereas, annual accumulation was taken as cumulated values.

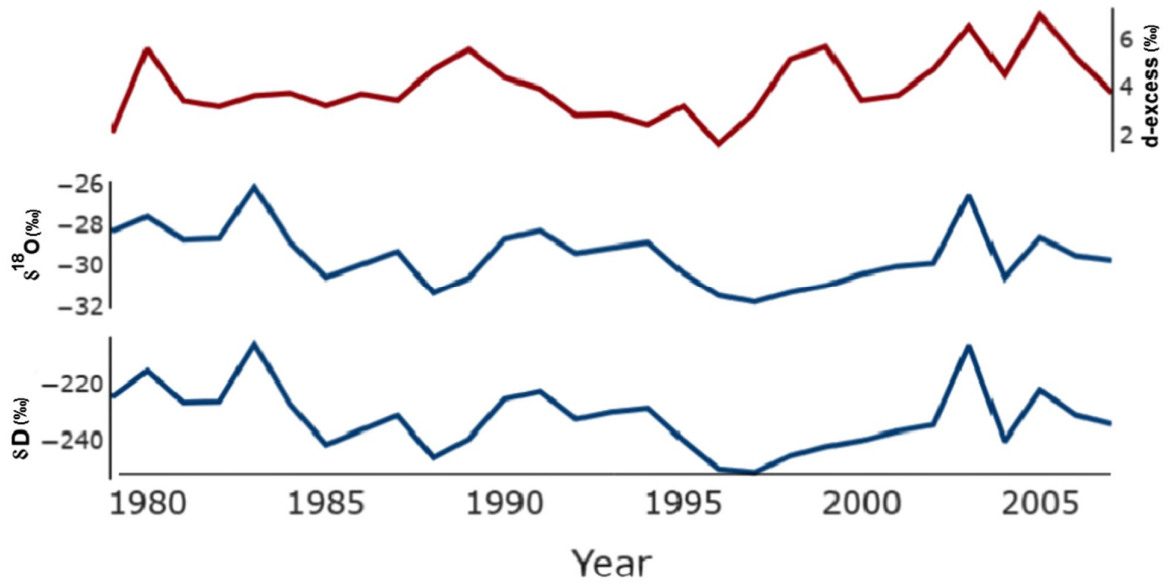

Fig.6.3.1- Annual isotopic temporal series for core B during 1979-2007.

Temporal series of core B (Fig. 6.3.1), showed a decreasing trend in the isotopic contents ($\delta^{18}O$, δD) during 1985-1990 and 1994-2004 while there is a short increase in $\delta^{18}O$ and δD during 1991-1994. Furthermore, 1983 and 2003 recorded with the highest mean annual isotopic contents. The temporal distribution of d-excess displayed an anti-phase behavior against $\delta^{18}O$ and δD in the inter-annual series which will be discussed in the later section of this thesis.

	Core B	Core D	Core E	Stacked Record
$\delta^{18}O$ (‰)				
Min	-31.89	-32.34	-30.62	-31.62
Max	-26.15	-27.72	-28.61	-27.29
S.dev	1.46	1.14	0.85	1.03
Mean	-29.50	-29.84	-29.73	-29.76
δD (‰)				
Min	-251.36	-252.97	-237.37	-247.62
Max	-205.61	-215.63	-225.94	-214.00
S.dev	11.94	9.3	5.35	8.92
Mean	-232.05	-233.52	-231.02	-233.51
d-excess (‰)				
Min	1.62	3.35	2.95	2.90
Max	6.96	6.13	6.14	5.94
S.dev	1.21	0.9	1.49	0.89
Mean	4.01	5.20	4.87	4.50

Table.6.3.1- Inter-annual isotopic values for GV7.

Although there is periodic trending in isotopic values in all the 3 ice cores, yet the mean annual stable isotope values for $\delta^{18}O$ and δD fluctuate around -29.50 ‰ and -232.5 ‰, respectively (Table 6.3.1). The concordance of isotopic values of cores (B, D, E) and stacked records suggested, that there were similar influences of local atmospheric conditions over GV7. The standard deviation (σ) for $\delta^{18}O$ remained between 0.85-1.46, the latter belonging to core B; in the case of δD, a high standard deviation of 11.94 was recorded for core B.

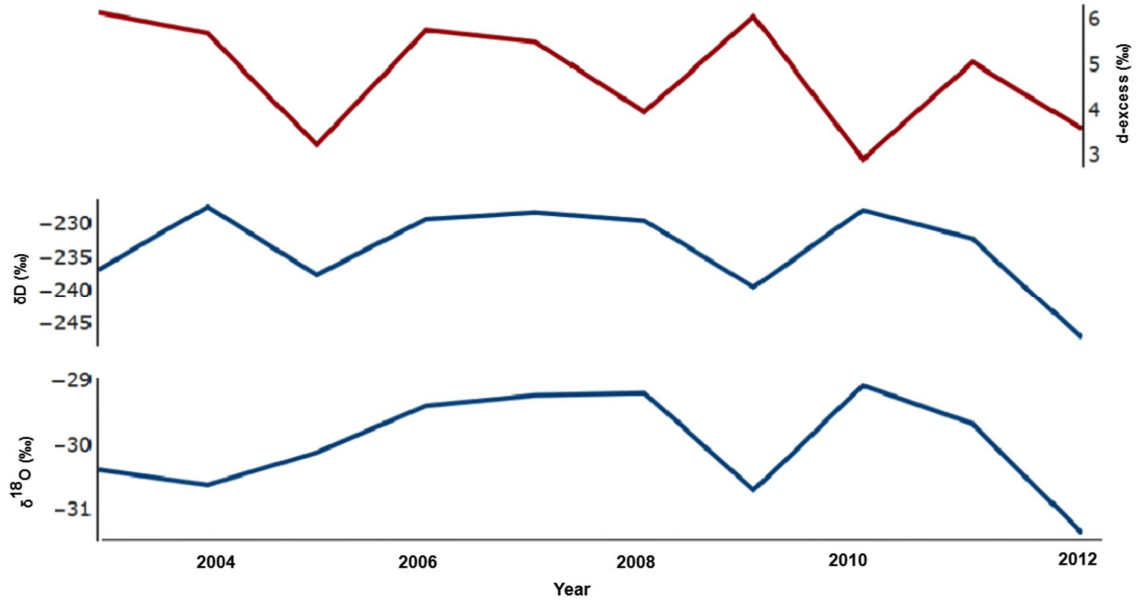

Fig.6.3.2- Annual isotopic temporal series for core E during 2003-2012.

We observed a similar increasing trend $\delta^{18}O$ and δD values in core E and D (not shown) for the period 2003-2012 and 1990-2002 respectively. The temporal series of isotopic values from cores and stacked records (Fig.6.3.3), suggested, that 1983, 1991 and 2003 were recorded with less depletion of $\delta^{18}O$ while 1988, 1997-98, 2009 and 2012 displayed highly depleted values.

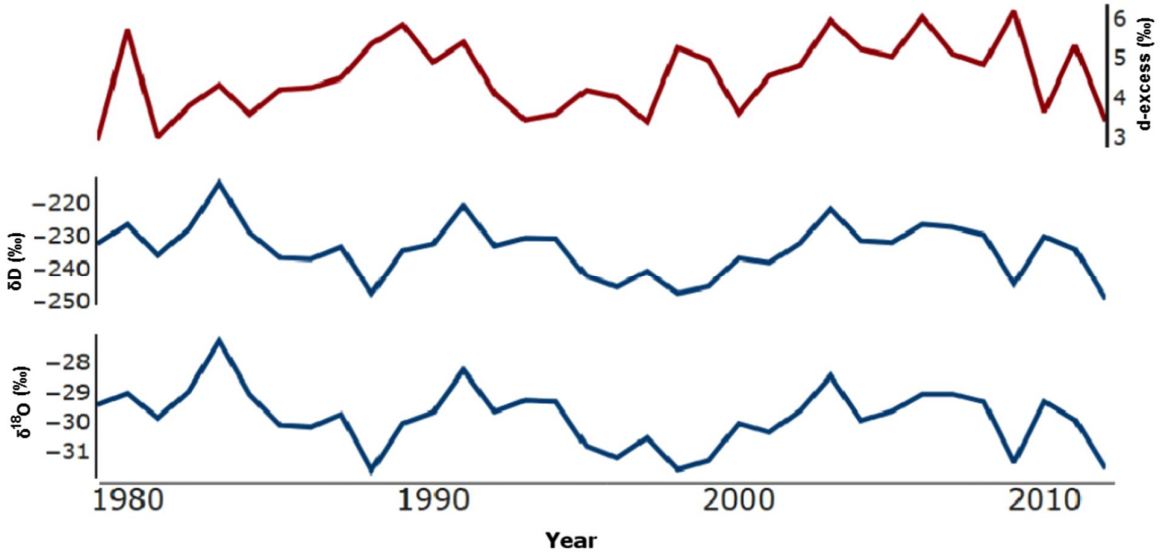

Fig.6.3.3- The stacked record of GV7 produced from the mean annual values (stable-isotopes and d-excess) of core B, D, E, and ITASE 2001-2002.

6.4 Snow Accumulation Rate

Snow accumulation record in ice cores is the combination of precipitation, sublimation/evaporation, and deposition as a result of wind redistribution. It provides adequate information (annual-decadal-centuries), for trend evaluation (Thomas et al., 2017). A composite accumulation time series was constructed analogously for each ice core individually and stacked record which analyzed for the corresponding period of each ice core. The data of snow accumulation rate used in all correlations in this thesis ha been provided by Claudio Scarchilli at ENEA (Rome).

We obtained the core depth in snow water equivalent (w. e.) using the density of GV7 cores, with the following equation

$$SWE = HS \cdot \rho$$

Where SWE is the depth in snow water equivalent, HS is the length of the depth interval (cm) and ρ is the density (kg/m^3).

The annual snow accumulation rate (cm. we), at GV7 cores (B, E) disclosed a good agreement with the stacked record while there was an insignificant increase recorded in core D. However, there was a considerable change in the standard deviation of core B (12.6), as compared to core D, E and stacked record (8.70, 7.52 and 5.03 respectively).

The temporal distribution of snow accumulation from cores and stacked records were found in strong agreement showing high peaks of accumulation for 1983, 1992 and 1998. The annual accumulation rate of core D in 1991 is considerably low where it was recorded as one of the highest years of snow accumulation for core B and stacked record. We assume, that there could be post-depositional processes, which resulted in the re-distribution of snow at the point where core D retrieved. The snow accumulation for a given site can differ from the regional or local average due to uneven topography and post-depositional processes (Wang et al., 2016). Therefore, a composite record is necessary to reduce the modification caused by these processes.

Table. 6.4.1- Annual snow accumulation rate (cm. we) at GV7.

	Core B	Core D	Core E	Stacked Record (GV7)
Minimum	23.01	15.08	12.42	15.11
Maximum	32.14	54.31	31.97	36.03
Standard deviation	12.6	8.70	7.52	5.03
Mean	23.01	25.71	22.83	23.87

Atmospheric reanalysis data are key to understand the local and regional accumulation variability (Cohen and Dean., 2013).

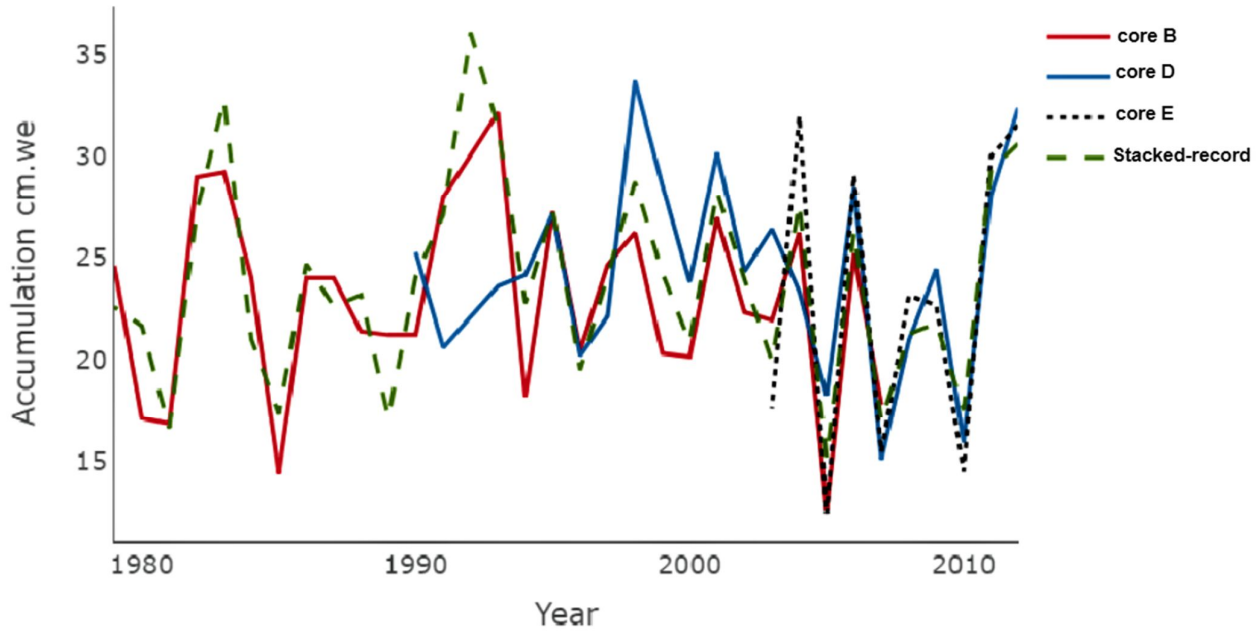

Fig.6.4.1- Annual snow accumulation (cm. we) at GV7 along with the stacked record.

For this research study, we used state-of-the-art ECHAM5-wiso and ERA-Interim for obtaining the temporal distribution of precipitation over the GV7 site during 1979-2012. Precipitation is one of the dominant terms for several different components (precipitation, sublimation/vapor deposition, and snowdrift) of snow accumulation (Bromwich and Zhichang, 2004). ERA-Interim Precipitation-Evaporation (P-E) is considered the key to showing reliable inter-annual variability of precipitation (Wang et al., 2017).

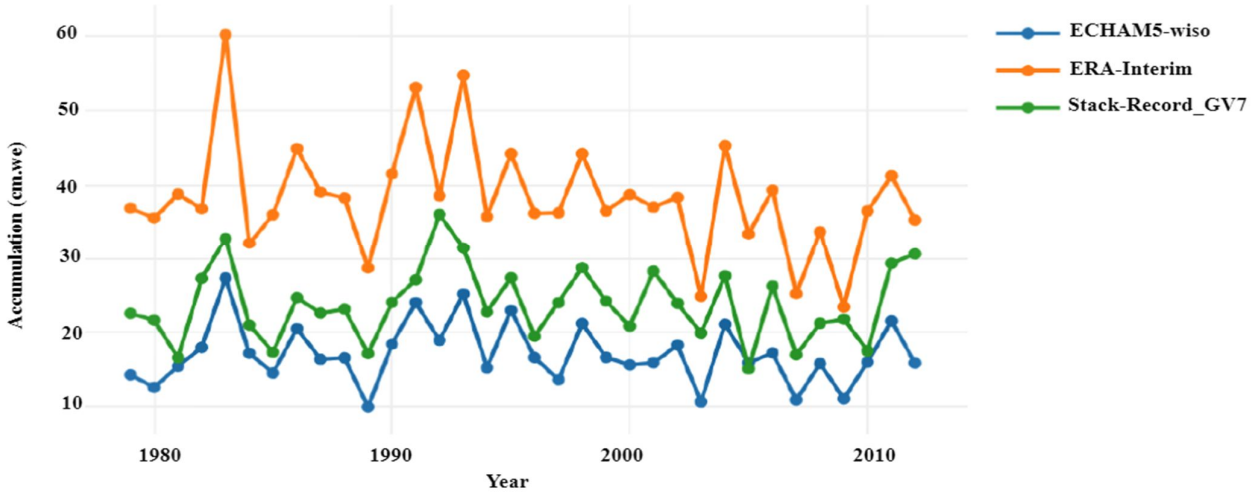

Fig. 6.4.2- Temporal distribution of accumulation/precipitation from ice records and re-analysis data from 1979-2012 for GV7.

Since the stacked record showed striking similarities with individual records (Fig. 6.4.1), therefore, we addressed stacked accumulation records for comparison purposes. Precipitation records from the ECHAM5-wiso model and the stacked record of accumulation from GV7 showed strong in-phase agreement excluding the last 4-5 years of the specified time period. Moreover, in the quantitative comparison, we observed the over-estimation of precipitation records from ERA-Interim (38.23 cm yr^{-1} annual average), with net increase of 52.62 %, while precipitation records from ECHAM5-wiso (i.e. 17.11 cm yr^{-1} mean annual) underestimated as compared to accumulation stacked-record which is 23.87 cm. we

(mean annual) showing a decrease of 30.34 %. Additionally, the accumulation record from cores data suggested a highly significant correlation with precipitation records from ECHAM5-wiso and ERA-Interim (Table.6.4.2). We noticed a marginally small increasing trend in cores accumulation records while in the precipitation temporal distribution showed small-to-large (ECHAM5 and ERA-Interim respectively) decreasing trend post-1990. The in-phase agreement and significant correlation of ice core accumulation records with ECHAM5-wiso and ERA-Interim precipitation records suggested that we obtained a robust temporal resolution in our data.

6.5. Correlations

In this section, we present the correlations between observed data from ice cores (stable isotopes and accumulation) and the simulated data from Atmospheric General Circulation Model (AGCM), ECHAM5-wiso and ERA-Interim. Before model-data comparison, we took the 3-year moving average to avoid any stratigraphic noises. Furthermore, we could not find any significant correlation between model-simulated stable isotopes and observed stable isotopes, therefore, we calculated the precipitation-weighted stable isotopes (onward as $\delta^{18}O_p$ and δD_p), as well as the precipitation-weighted temperature of simulated data (model data). In the case of core E, we could not find any significant correlations between observed and simulated stable isotopes data.

Table. 6.5.1- Correlations between observed (cores) and simulated data (model) from 1979-2012.

	ECHAM5-wiso				ERA-Interim	
Observed Data	**Precipitation ($cm.y^{-1}$)**	**$\delta^{18}O_p$ (‰)**	**δD_p (‰)**	**Temperature $_p$ °C**	**Precipitation ($(cm.y^{-1})$)**	**Temperature °C (T 2m)**
Core B Accumulation	r^2=0.69 p-value<0.0001 slope= 0.86				r^2= 0.64 p. value<0.0001 slope= 0.45	r^2=0.22 p. value= 0.008 slope= 2.51
$\delta^{18}O$ (‰)		r^2=0.42 p.value= 00012 slope=1.22	r^2= 0.45 p.value<0.0001	r^2= 0.38 p-value= 0.00035 slope=0.57		
δD (‰)		r^2=0.43 p. value=0.0001 slope=9.98	r^2= 0.46 p. value<0.0001	r^2=0.36 p. value=0.0006 slope=4.46		
Core D Accumulation	r^2=0.35 p. value=0.002 slope=1.15				r^2=0.33 p. value=0.003 slope=0.54	
$\delta^{18}O$ (‰)		r^2=0.30 p. value=0.007 slope=0.89	r^2=0.33 p.value=0.004	r^2= 0.25 p.value= 0.02		
δD (‰)		r^2=0.30 p. value=0.006 slope= 7.69	r^2=0.34 p. value= 0.004	r^2=0.23 p.value= 0.02		
Core E Accumulation	r^2= 0.40 p. value=0.05					
Stacked-Record Accumulation	r^2=0.53 p. value<0.0001				r^2=0.41 p. value<0.0002	r^2=0.13 p. value=0.03 slope= 2.23
$\delta^{18}O$ (‰)		r^2=0.47 p. value<0.0001	r^2=0.51 p.value<0.0001	r^2=0.31 p. value=0.0005		
δD (%)		r^2=0.45 p. value<0.0002	r^2= 0.50 p. value<0.0001	r^2=0.27 p. value=0.001		

Table.6.5.2- Correlation table of d-excess (‰) relative to sea ice extent (SIE) and stable isotope

	Western SIE			Indian SIE			Ross SIE		
	r^2	*p-value*	*correlation*	r^2	*p-value*	*correlation*	r^2	*p-value*	*correlation*
Core B									
Deuterium excess				0.38	0.00083	Positive			
$\delta^{18}O$ (‰)							0.57	<0.0001	Negative
Core D									
Deuterium excess	0.32	0.005	Negative						
$\delta^{18}O$ (‰)							0.38	0.002	Negative
Core E									
Deuterium excess	0.44	0.04	Negative	0.78	0.0006	Negative			
$\delta^{18}O$ (‰)	0.49	0.02	Positive						
Stack Record									
Deuterium excess	0.12	0.02	Negative	0.18	0.01	Positive	0.23	0.004	Positive
$\delta^{18}O$ (‰)							0.31	0.0006	Negative

7 Discussion

7.1 Deuterium excess and $\delta^{18}O$ phase correlation

Previous studies have documented the spatial variations of d-excess in Antarctica, yet the temporal variations are poorly recorded and understood (Goursaud et al., 2019). At high-latitudes, unlike annual cycles of $\delta^{18}O$ and δD, d-excess has summer minima and winter maxima.

Our findings displayed that d-excess appeared to be anti-correlated with $\delta^{18}O$ with a slope of (-0.05) for the stacked record (Fig. 7.1.1). We performed the same exercise for all ice cores and found a similar correlation between d-excess and $\delta^{18}O$. Although there is strong consensus about systematic biases of model approach for d-excess, yet the model captured the anti-phase correlation of $\delta^{18}O$ and d-excess with a slope of (-0.15), which is 3 times weaker than the observed d-excess and found in agreement with the precipitation record of Concordia station, East Antarctica (Stenni et al., 2016).

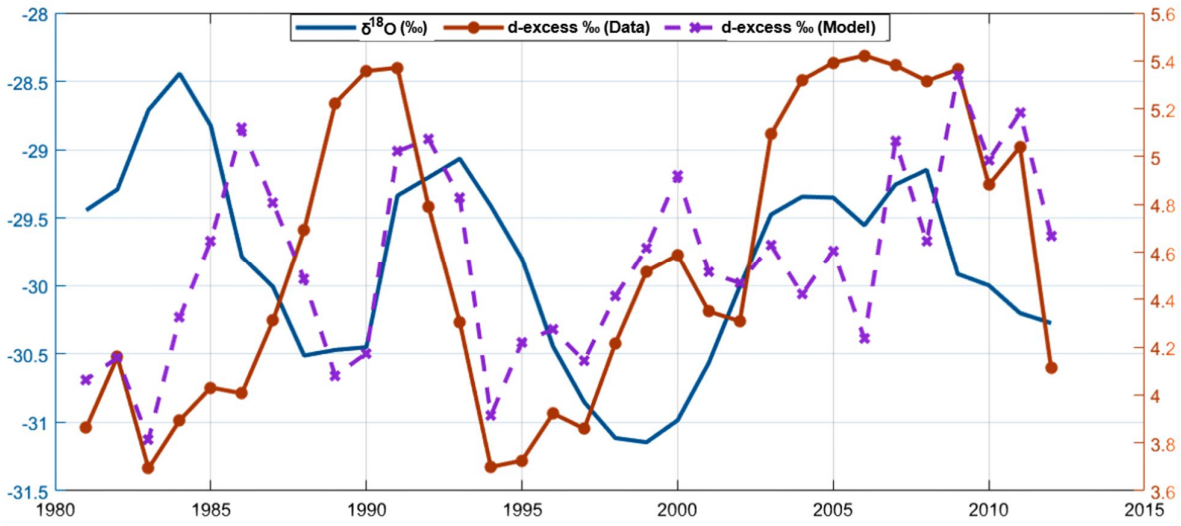

Fig 7.1.1- Inter-annual variation of d-excess and $\delta^{18}O$ from the stacked record with a moving mean of 3 years. We also address the d-excess variations from the ECHAM5-wiso model. The difference between the d-excess (a stacked record) and ECHAM5-wiso variations shows the biased skills of the model. One of the possible reasons is that ECHAM5-wiso is not equipped with humidity which is one of the controlling factors of d-excess.

In order to understand any post-depositional processes that had taken place, we applied a simple approach to quantify variations in seasonal amplitude of d-excess and $\delta^{18}O$ as an indicator of post-depositional smoothing, illustrated by Goursaud et al. (2019).

We calculated the average ratio of the first 3 seasonal cycles of d-excess and $\delta^{18}O$ as well as the average of d-excess and $\delta^{18}O$ through the entire time period (1979-2012) for all cores.

In the case of any large post-depositional smoothing, the calculated ratio should be greater than 1. While we found a ratio ranges from 0.78-to-1 for $\delta^{18}O$ and 1-to-1.27 for d-excess.

The calculated ratios from our data suggested that no large post-depositional processes had taken place and that seasonal cycles remained stable through time. Furthermore, we found strong summer minima and winter maxima in the d-excess seasonal cycle (Fig. 7.1.2). This anti-phase behavior of d-excess with $\delta^{18}O$ should be analyzed in-depth to understand the potential seasonal lagging of d-excess as various studies documented (e.g Stenni et al., 2016, Aizen et al., 2005). To study this methodology here is beyond the scope of this study.

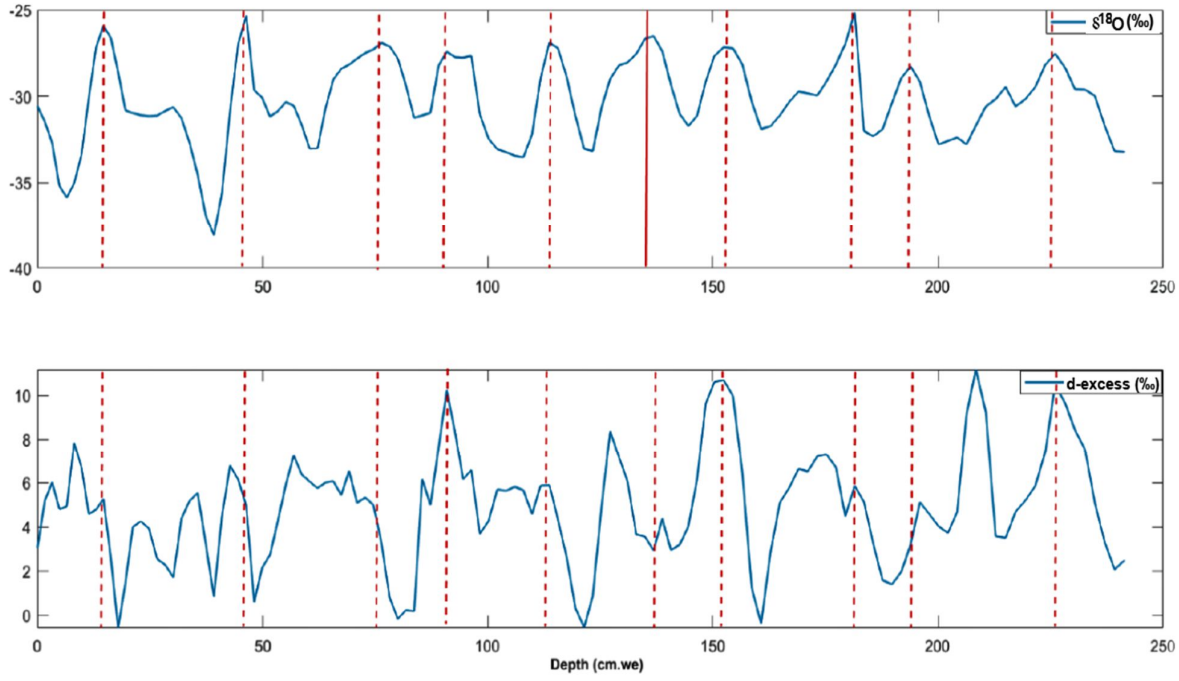

Fig. 7.1.2- The seasonal amplitude of d-excess and $\delta^{18}O$ of core E (2003-2013). Strong winter maxima and summer minima of d-excess. There could be more than one maximum in a single year.

7.2 Comparison between ice cores and model (ECHAM5-wiso & ERA-Interim) data

7.2 .1 Comparison of observed and modeled $\delta^{18}O$

In order to provide a climatic interpretation of stable water isotopes with a better physical basis, we used Atmospheric Global Circulation Model (AGCM) nudged to ERA-Interim, which is equipped with isotopes tracers (e.g Goursaud et al., 2018). For this analysis, we calculated the annual mean values of $\delta^{18}O$ and δD (not shown) as precipitation weighted means (addresses as $\delta^{18}O_p$ onward). To avoid any stratigraphic noises, we filtered simulated (model data) and observed (ice cores) data with 3 years moving average. Since, in the stacked record, we retained the same signal as individual ice and firn cores, therefore we use the stacked record as observational data for this analysis.

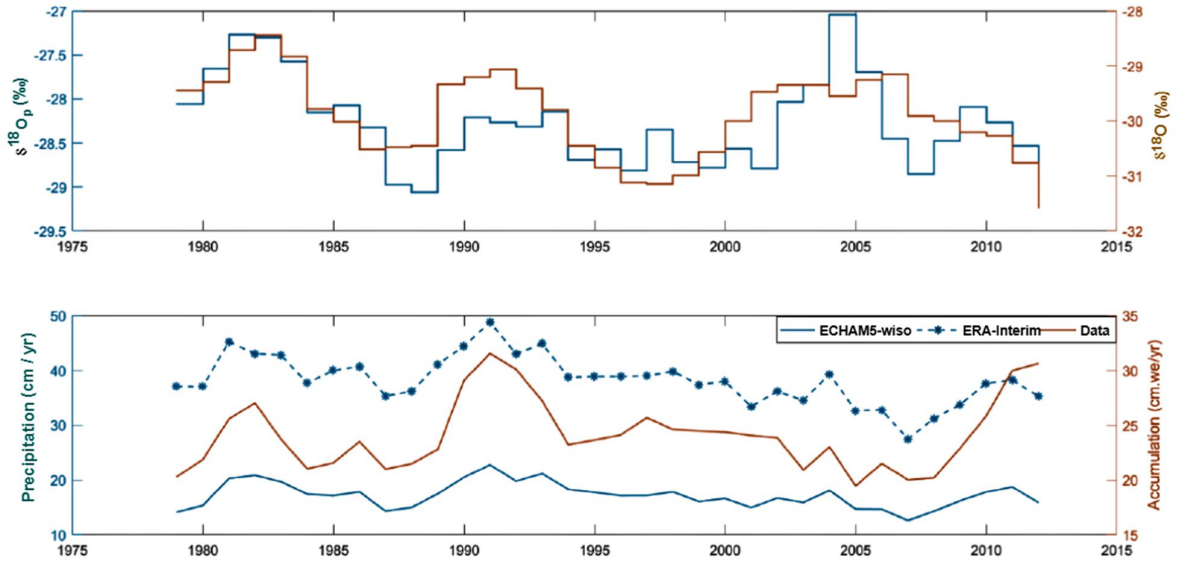

Fig. 7.2.1.1- Comparative analyses of observed-model (ECHAM5-wiso and ERA-Interim). The top graph shows the comparison between precipitation-weighted $\delta^{18}O_p$ vs observed $\delta^{18}O$ while graph (bottom) shows the temporal distribution of model-simulated precipitation vs observed accumulation annual rate during 1979-2012.

We found a strong linear correlation (r^2= 0.47, p.value< 0.0001, slope= 1.03) of simulated $\delta^{18}O_p$ temporal variations with observed $\delta^{18}O$ values from (1979-2012). However, the simulated $\delta^{18}O_p$ (-28.38‰) overestimated observed $\delta^{18}O$ (-30.03‰) by 5.51 % (Fig.7.2.1.1). The overestimation of $\delta^{18}O_p$ in coastal Antarctica has been previously addressed by (Goursaud et al., 2018). We found a similar correlation for core B and D (not shown) while no significant relationship noticed in core E.

	ECHAM5-wiso				ERA-Interim	
	Precipitation (cm/yr)	**$\delta^{18}O_p$ (‰)**	**Temperature °C (T p)**	**d-excess (‰)**	**Precipitation (cm/yr)**	**Temperature °C (T 2m)**
Min	9.95	-29.87	-32.52	3.81	23.46	-26.38
Max	27.33	-26.18	-25.40	5.34	60.20	-23.17
Mean	17.12	-28.27	-29.04	4.54	38.28	-24.40
St.dev	4.10	0.88	1.91	0.39	7.80	0.76

Table 7.2.2.1- Precipitation, Temperature, $\delta^{18}O$ and d-excess values from ECHAM5-wiso and ERA-Interim. Temperature and $\delta^{18}O$ values have been taken as precipitation weighted (as T_p and $\delta^{18}O_p$ respectively).

7.2.2 Comparison between accumulation and precipitation

We used the precipitation record from ECHAM5-wiso and ERA-Interim to obtain a robust temporal resolution of accumulation records from ice cores data. We noticed, that there is a strong resemblance between the simulated precipitation from models and accumulation records from observed data (Fig 7.2.2.1). We obtained a strong linear correlation between accumulation records from ice cores stacked record (except core E) and precipitation data from models ($r2= 0.53$, $p.value<0.0001$). However, precipitation records from ERA-Interim show a large over-estimation of 52.62 % with a mean annual value of 38.28 cm/yr (Table 7.2.2.1) while ECHAM5-wiso shows under-estimation of 30.34 % with mean annual value of 17.2 cm. when compared to observed accumulation data. We performed the regression analysis for $\delta^{18}O_p$ -accumulation relationship, where ECHAM5-wiso failed to capture any significant correlation. The recent monitoring of surface snow and surface vapor isotopic composition in polar regions revealed the possible exchange between surface snow and water vapor during snowfall events (Ritter et al., 2016; Steen-Larsen et al., 2014), but these processes are not accounted in the atmospheric models. Therefore, in this study, we used precipitation weighted $\delta^{18}O_p$. We assume that the over-estimation of the model's

isotopic data is associated with the local post-depositional processes. Katabatic winds can produce local atmospheric effects such as the re-distribution of freshly fallen snow and result in isotopic depletion. Since atmospheric models are only capable to capture the regional atmospheric effects (and not local atmospheric effects), therefore the isotopic depletion associated with the local post-depositional process is not noticeable in the model's data.

We also suggest that challenges associated with model skills at ocean boundary could be another reason for the model-data mismatch. Besides, quantitative mismatch of model-data isotopes and precipitation-accumulation comparison, there is a strong in-phase resemblance between observed and simulated stable isotopes model-data variations, which suggest a clear synoptic deposition (e.g. Goursaud et al., 2018).

7.2.3 Accumulation sensitivity to near-surface temperature

In our study, we also considered the importance of near-surface temperature (T_{2m}) in shaping the accumulation pattern over the GV7 site. We performed a linear regression analysis between near-surface temperature extracted from ERA-Interim and accumulation records from ice cores data. Snow accumulation is dependent on a few factors i: e elevation, distance from the coast and temperature. Since the study site is in coastal Antarctica with comparatively less elevation than inland Antarctic plateau, which controls the annual accumulation, therefore we only run a linear regression for finding the correlation between near-surface temperature and accumulation.

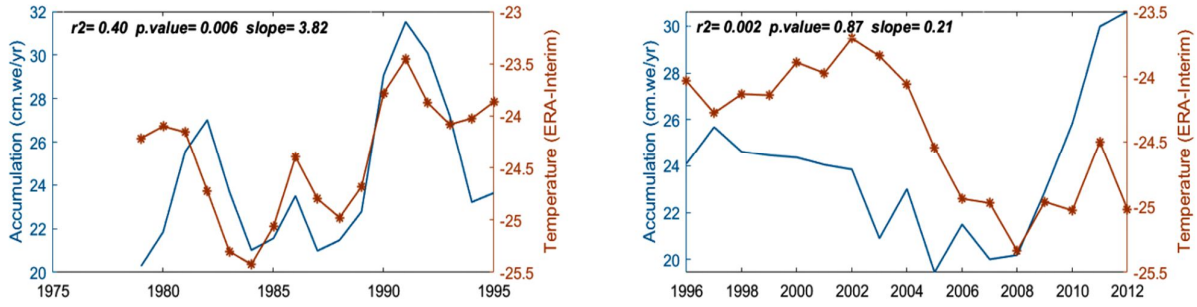

Fig. 7.2.3.1- Stacked record accumulation sensitivity to near-surface temperature (T_{2m}) extracted from ERA-Interim. Records have been split into two time periods to understand the earlier (left side) and recent (right side) accumulation pattern as a function of near-surface temperature. Accumulation and temperature remained co-variant until 1995 and appeared to be dephased onward.

Several studies (Monaghan & Bromwich, 2008, Medley et al., 2017), recorded warmer temperatures with increased accumulation.

We found a strong linear correlation between ERA-Interim near-surface (T_{2m}) temperature and the accumulation from the stacked record. We also observed a fair co-variance between near-surface temperature and accumulation from 1979-1995 (7.2.3.1 left side), with a correlation coefficient of r^2=0.40, however, no significant correlation was noticed during 1996-2012 (Fig.7.2.3.1. right side) and appeared to be dephased after 1995. We found good correlation (r^2= 0.22, p.value= 0.008) in core B (not shown) for its entire period (1979-2007) but no significant relationship (accumulation-temperature) found in core D and E.

7.2.4 δ^{18}O-Temperature (δ-T) relationship

In order to understand the empirical relationship of δ^{18}O and temperature**,** we used the near-surface temperature extracted from ERA-Interim and ECHAM-wiso model and δ^{18}O from ice cores data. The average surface temperature (T_{2m}°C), as well as precipitation-weighted temperature (T_p °C), simulated by ECHAM5-wiso, showed a good correlation with observed stable isotopes.

δ^{18}O (‰)	**r^2**	**p.value**	**Slope**
Core B	0.33	0.001	0.26
Core D	0.29	0.008	0.31
Stack-Record	0.19	0.01	0.24

Table 7.2.4.1- Annual correlations between average temperature extracted from ECHAM5-wiso and δ^{18}O (‰) reconstructed from ice cores data.

The linear regression between the observed δ^{18}O and ECHAM5-wiso simulated average temperature during 1979-2012 demonstrated good correlation (Table 7.2.4.1) with a slope ranged from 0.24 to 0.31 (Fig. 7.2.4.1). We could not detect any significant correlation in the shallow firn core E. we assume that the

shallow depth profile of core E could make it more vulnerable to wind scouring and other post-depositional process, which can result in depleted isotopic values. Additionally, the model could also fail to capture any true isotopic signal due to its biased performance in the coastal regions.

There was found a strong correlation between the precipitation-weighted temperature (T 2m $_{p}$) and $\delta^{18}O$ (Table.6.5.1). We observed a stronger correlation with high significance level in stacked record (r^2= *0.31, p.value=0.0005, slope= 0.74*), core B (r^2= *0.38, p.value= 0.0003, slope=0.57*) and core D (r^2=0.25, p.value=0.02, slope= 0.63). However, we could not find any significant correlation between the observed $\delta^{18}O$ and ERA-Interim simulated near-surface temperature (T 2m $_{surf}$). We assume that simulated temperature from ECHAM5-wiso is closer to the condensation temperature of the study site than ERA-Interim (Goursaud et al., 2017).

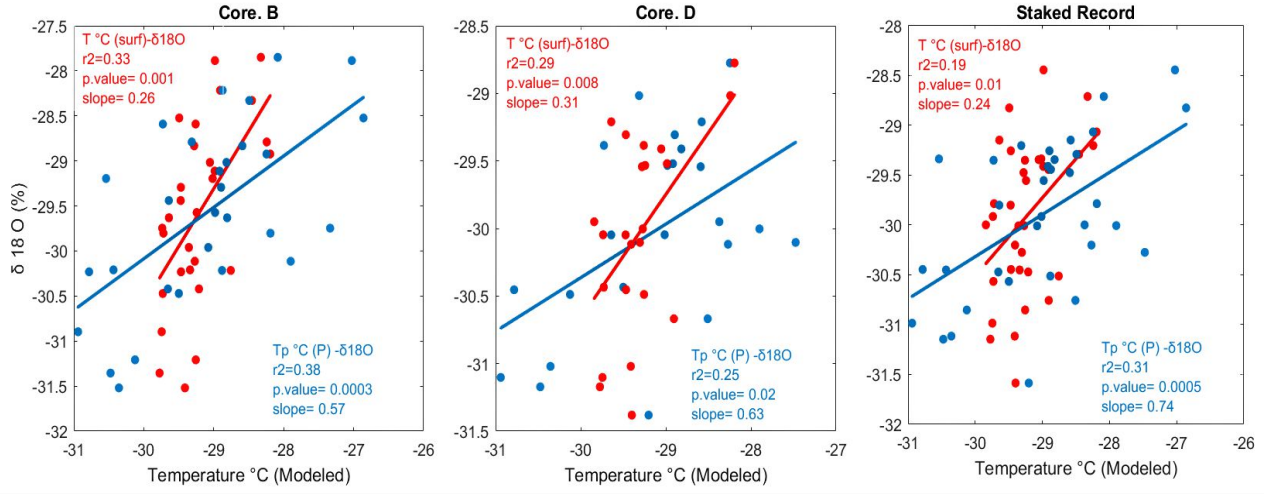

Fig.7.2.4.1- Variations of observed stable isotopes ($\delta^{18}O$) as a function of simulated Temperature. (Red) represents the slope between Surface Temperature (T°C surf) simulated by ECHAM5-wiso while (Blue) plot shows the observed stable isotopes as a function of Precipitation weighted Temperature (T p°C).

We made a composite record of ice and firn cores to eliminate any signal-to-noise fluctuations in our results. We assume that the ERA-Interim model does not possess the skills to capture moisture transport pathways causing variabilities in the precipitation signal. We propose that model-data comparison in coastal Antarctic sites should be analyzed more carefully due to biased records of atmospheric models in coastal Antarctica especially when dealing with data from shallow firn cores.

7.2.5 Influence of sea ice extent on d-excess (moisture source proxy)

Although Antarctic ice sheets have expanded during the last few decades (at least until 2014), there is significant interannual variability of the sea ice extent, which can affect the hydrological cycle. Since d-excess is a moisture source proxy, it helps in understanding the change in the hydrological cycle of Antarctica due to sea ice loss (Klein and Welker, 2016).

The controlling factors behind d-excess are still needed to be fully understood. Sea ice extent is considered one of the controlling factors of d-excess, but it is still not concluded whether the d-excess correlation with the sea ice extent is positive or negative. Different studies (e.g. Kopec et al., 2015, Goursaud et al., 2019), observed different relationships (positive and negative) with sea ice extent (SIE).

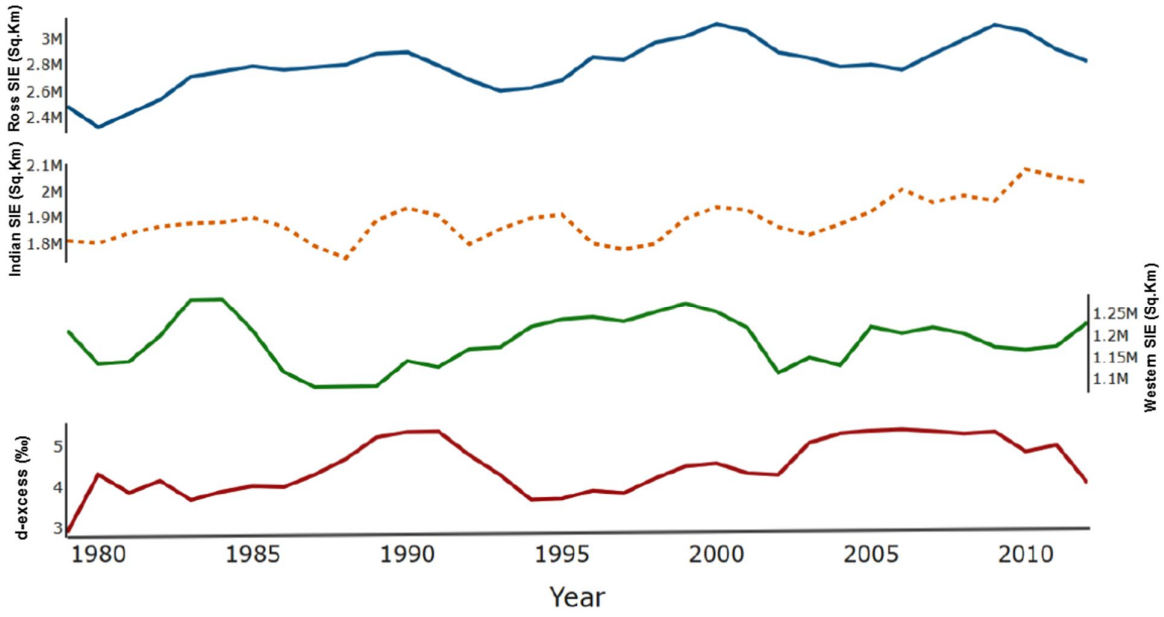

Fig.7.2.5.1- Deuterium excess values from the stacked record of GV7 against Ross Sea Ice, Indian Sea and WPO ice extent (measured in Square Kilometer). All values are shown in a 3-year moving average to avoid any outliers and missing data.

The Western Pacific sector is the major source of precipitation in GV7. We found an anti-correlation ($p<0.0075$, $r^2=0.20$) of d-excess with the WPO ice extent. We undertook the same exercise with the ECHAM5-wiso d-excess and the Western Pacific Ocean (WPO) ice extent, where we found an r^2 of 0.24; the correlation is significant (p.value=0.003), showing anti-correlation between sea ice extent (WPO) and d-excess (ECHAM5-wiso model). It is also worth mentioning that the WPO displayed a decreasing trend

in the sea ice extent post-1999-2000, while d-excess during this period showed an increasing trend. However, d-excess and sea ice extent both showed an increasing trend for the overall period of 1979-2012. We suggest that changes in sea ice extent over a long period of time might not influence the d-excess. Yet, a relatively small reduction in seasonal sea ice loss can result in higher d-excess values.

7.3 Signature of El Niño-Southern Oscillation in GV7

The ice core data carries the potential to help in understanding the El Nino-southern oscillation impacts over the Antarctic climate (Turner, 2004). The El Niño/Southern Oscillation (ENSO) is a naturally occurring phenomenon that involves fluctuations of the central and eastern equatorial Pacific, coupled with changes in the atmosphere (Wang et al., 2016). ENSO and La Nina conditions occur 31% and 23% respectively while the remaining 56% is the neutral phase. (Welhouse, 2016).

In this research work, we studied the ice cores and model reanalysis data from the GV7 for a possible connection with El Nino during 1979-2012. For this purpose, we used the model reanalysis data from two different atmospheric models i: e ECHAM5-wiso and ERA-Interim.

In order to understand the consistent effects of ENSO 3.4, it is particularly important to study the precipitation variability of coastal eastern Antarctica. Therefore, we compared the variabilities of accumulation history as well as modeled precipitation data (not shown) from ECHAM5-wiso relative to ENSO 3.4 events. The accumulation record from the core (B) showed weak correlation (*r2=0.21, p.value=0.01*) with ENSO 3.4, while no significant correlation was found in stacked record and core D. However, the simulated precipitation was found in good correlation *(r2=0.26, p.value=0.006)* with ENSO 3.4 (Table 7.3.1). It is understood that ENSO effects are not only limited to SST, but it is also one of the dominant modes of atmospheric variabilities. The simulated precipitation from atmospheric models suggests that ENSO 3.4 had influenced the atmospheric modes of variability in this part of Antarctica.

The years 1981-82 and 1990-93, were observed with the maximum increase in accumulation, which found in accordance with high ENSO values during the same years.

Furthermore, we studied the surface temperature using ECHAM5-wiso and ERA-Interim reanalysis data.

It was noticed that temperature re-analysis data from ERA-Interim was found in a weak positive correlation with ENSO 3.4, while ECHAM5-wiso simulated temperature showed a highly significant correlation (table 7.3.1). It was also noticed that re-analysis surface temperature showed comparatively stronger anomalies during ENSO 3.4 years until 1991-92 but afterward, the overall temperature had downward trend despite showing resemblance with ENSO 3.4 peaks.

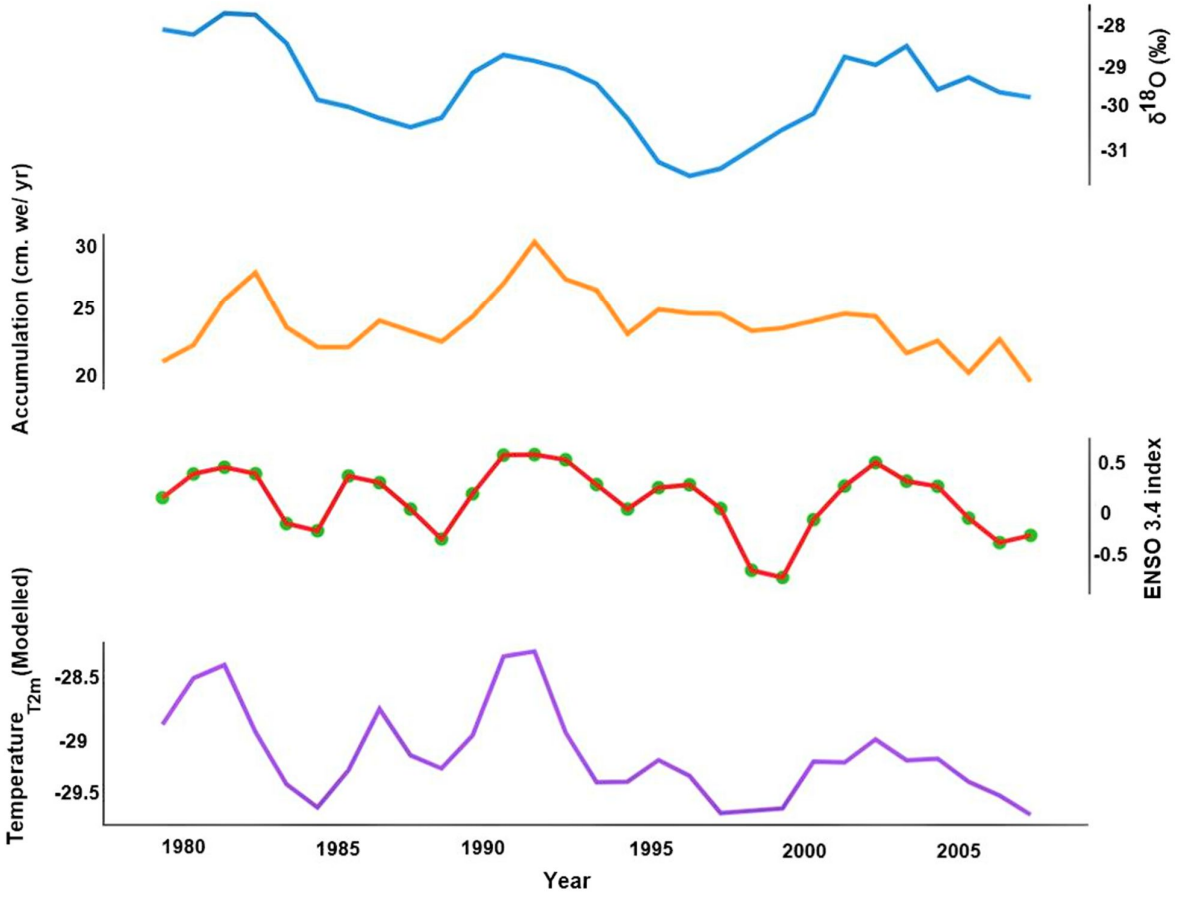

Fig.7.3.1- Ice core (B) accumulation and $\delta^{18}O$ anomalies relative to ENSO 3.4 events as well as the response of simulated surface temperature during 1979-2007.

We assume that though the surface temperature had been responsive to ENSO 3.4 events, yet the long term decreases post-1991 indicated, that ENSO could not be a key driving force in determining the surface temperature anomalies in this part of Antarctica. We further explain this by observing the years with lowest surface temperature recorded following strong ENSO years. Since we found a strong correlation of δ-T

relationship in earlier statistical comparison between model and observed data, therefore to further infer ENSO signal, we also considered stable isotopes data from ice cores relative to ENSO 3.4. The cores (B and D) stable isotopic contents were found in a weak correlation with ENSO. However, the composite stacked record from ice cores enhances the correlation strength between stable isotopes and ENSO (Table7.3.1). Moreover, the precipitation weighted $\delta^{18}O_p$ showed the same correlation strength with ENSO during 1979-2012. We assume that the atmospheric circulations of Antarctica had been responsive to ENSO events.

	r^2	*p. value*	*slope*
Core B $\delta^{18}O$ (%)	0.21	0.01	0.16
Core D $\delta^{18}O$ (%)	0.25	0.02	0.26
Stacked record $\delta^{18}O$ (%)	0.22	0.005	1.02
Core B Accumulation (cm. we. y^{-1})	0.28	0.003	0.07
Precipitation (ECHAM5-wiso)	0.24	0.006	0.07
Temperature $_{surf}$ (ECHAM5-wiso)	0.56	<0.00001	0.57
Temperature $_{T\ 2m}$ (ERA-Interim)	0.21	0.01	0.31

Table 7.3.1- ENSO effects on stable isotopes and accumulation in ice cores and stacked records. The model reanalysis data of precipitation and temperature (near-surface) were also investigated.

We also observed that model simulated temperature showed weak positive anomalies to strong ENSO events during 1995-2007 (Fig. 7.3.1) with a standard deviation of 0.25°C y^{-1} which drop down from the standard deviation of 0.47 °C y^{-1} during 1979-1994. On the other hand, $\delta^{18}O$ from ice cores had been strongly responsive (standard deviation 0.93) relative to ENSO events during 1979-2007.

We assume that the weak response of surface temperature relative to ENSO 3.4 indicated that ENSO events

in this part of the Antarctic had not been the major contributor to the variabilities of surface temperature post-1990-91

From the discrepancies of temperature (simulated) and stable isotopes (from ice cores) relative to ENSO 3.4 anomalies, we assume that the atmospheric model rather captures the regional temperature signal, whereas, variabilities of isotopic contents could be more in response to local atmospheric events than regional near-surface temperature. This could be further explained by the $\delta^{18}O$-precipitation relationship where the local precipitation can result in the enrichment of stable isotopes.

Although our data from ice cores and atmospheric models showed compelling evidence of ENSO signature, yet it is hard to find the possible teleconnection of tropical based El Nino signature in Antarctic ice cores, as it is one of the debated atmospheric and oceanic processes. However, Hoskins and Karoly (1981), studies suggested that the area of deep convection near the equator produces Rossby waves, which act as a medium to propagate the increased tropical SST towards the southern hemisphere.

7.4 Effects of Antarctic Annular Mode on temperature and water stable isotopes

Alongside ENSO, another hemisphere-wide atmospheric phenomenon that influences the atmospheric variabilities and sea level pressure is Annular Mode. Unlike ENSO, the Antarctic Annular mode keeps its existence between mid and high latitudes. AAO in its positive phase brings cold towards eastern Antarctica by strengthening the westerlies winds resulting in lower air temperature while its negative mode towards the equator, creates lower pressure over the South pole and incoming warm air currents increase the air temperature.

The temperature variations relative to different modes of AO reflect in the ice core records. In order to investigate the influence of AO on stable isotopes and near-surface temperature, we used $\delta^{18}O$ from ice cores and reanalysis temperature data from ECHAM5-wiso. We performed the regression analysis for individual ice and firn cores as well as the composite stacked record for the period of 1979-2012. There was found a good negative correlation (r^2= 0.38, p.value=0.001) between observed stable isotopes of core D and AAO with a standard deviation of 0.72 and 0.42 respectively for the period 1990-2012. However,

no correlation was noticed in core B and firn core E. We observed that the correlation strength became significantly weak (r2=0.14, p.value=0.02) in the stable isotopes stacked record while the standard deviation remains almost the same as recorded in the core D. In order to understand the substantial weakening of correlation in stacked record, we further perform a linear regression by splitting the data into two periods i: e 1979-1995 and 1995-2012 (Fig. 7.4.1).

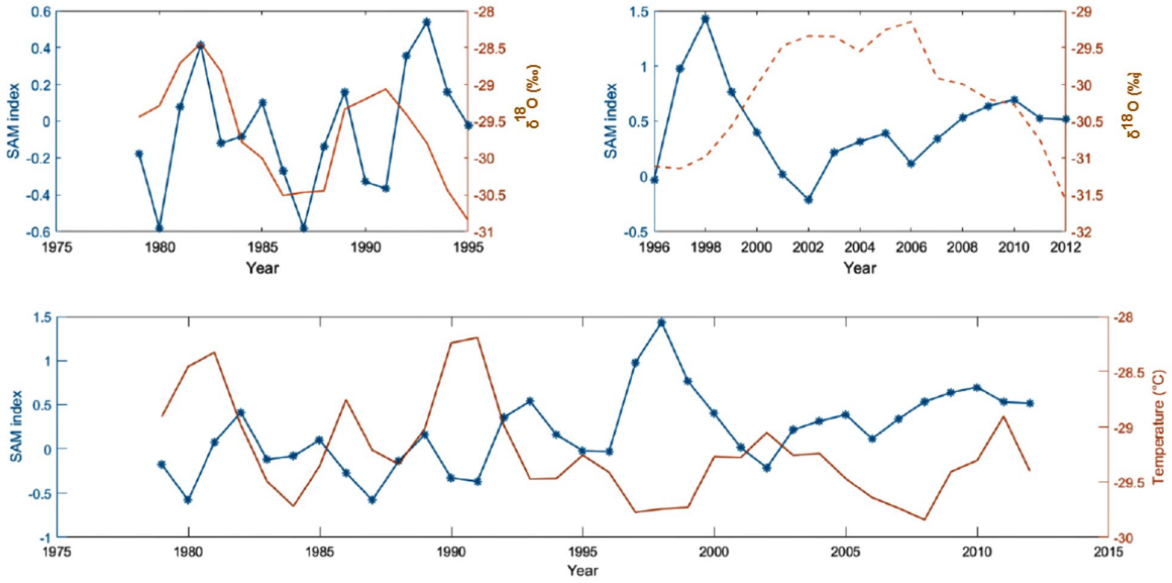

Fig.7.4.1- Regression analysis between AAO (SAM) and observed $\delta^{18}O$ for periods 1979-1995 and 1996-2012 (top) and variations of simulated air temperature relative to SAM events during 1979-2012 (bottom). Stable isotopes were used from the stacked record of GV7.

We performed the split periods' correlation considering that AAO is in a strong positive phase since 1995, which could possibly result in a strong correlation with stable isotopes records from 1995-2012.

After performing a regression analysis in split periods, we noticed a small increase in the correlation strength (r^2= 0.21) which indicates, that the recent positive phase of AAO is consistently influencing the variabilities of stable isotopes.

Furthermore, we investigate the simulated air temperature from ECHAM5-wiso relative to the Annular mode. There was found a good and highly significant correlation (r^2= 0.33, p.value=0.0004) between AAO and simulated air temperature with the same standard deviation of 0.43 for the period 1979-2012. Once

again, we performed the aforementioned split period comparison for calculating the increase (decrease) in observed $\delta^{18}O$, simulated air temperature, and AO during 1979-2012. It was found that during 1995-2012 (according to our analysis of stacked record), the AO index is showing an increase of 0.49 alongside the depletion of 0.50 % in the observed stable isotopes as well as 0.42 ℃ decrease in the simulated air temperature. We assume, that the weak correlation of stable isotopes and AO, could be because ENSO and AO influence the isotopic contents in a contrasting way. Therefore, the enrichment of $\delta^{18}O$ during ENSO events can be counterbalanced by the depletion of $\delta^{18}O$ during AO events. We further explained it by the correlation strength of ENSO and AO with $\delta^{18}O$ which are (r^2=0.22, p.value=0.005) and (r^2=0.14, p.value= 0.02) respectively. However, besides these climate indices, post-depositional effects such as wind scouring and snow drifting in freshly fallen snow, as well as the smoothing of isotopic signals with greater depth, can result in the variabilities of stable isotope contents. Considering simulated air temperature correlation with ENSO and AO, we assume that greater part of temperature variations is caused by coupling effects of (ENSO, AO) in this part of Antarctica which in turn influences the isotopic contents. In order to better understand the variations of stable isotopes contents and near-surface temperature in coastal Antarctica, the coupled effects of ENSO and AO can be helpful (e.g Naik et al., 2010), which we cannot perform here as it is beyond the scope of this study.

7.5 Variabilities in Accumulation, Stable isotopes and Temperature

It was previously suggested that there is a positive empirical relationship between temperature and accumulation in Antarctica (Masson-Delmotte et al., 2008). It is also understood that increased accumulation results in heavy isotopes enrichment and behave in parallel manners. Therefore, in this section, we tried to find a relationship of accumulation with simulated near-surface temperature and stable isotopes. We found a good and significant correlation between temperature and accumulation (Table 7.5.1). It was observed that the strength of the correlation of accumulation with simulated temperature from ECHAM5-wiso remained stronger than ERA-Interim for the same period.

However, in the case of core D, temperature from ECHAM5-wiso failed to show any correlation with accumulation but a strong co-variance is recorded between temperature from ERA-Interim and accumulation.

We assume that ECHAM5-wiso simulated temperature is closer to condensation temperature than ERA-Interim while in case of core D, it could be due to the more local dispersion of freshly fallen snow (at core D location) due to snow drifting or wind scouring. Moreover, we could not find any significant correlation in core E which again we assume could be due to the uneven freshly fallen snow distribution and unstable annual layers where there is high chance of snow dispersion and other post-depositional processes.

Accumulation	**r^2**	**p.value**	**slope**
Core B **1979-2007**	0.28	0.003	3.10
Core D **1990-2012**	0.30	0.006	4.12
Stacked record **1979-2012**	0.19	0.009	3.24

Table.7.5.1- Linear regression analysis of accumulation from ice cores and stacked record with simulated near-surface temperature from ECHAM5-wiso and ERA-Interim.

Furthermore, no significant correlation was observed for accumulation and stable isotopes. Interestingly, we noticed a contradictory shift in accumulation and stable isotopes after 1999-2000, when they appear in antiphase, while they remained in-phase before 1999 (Fig.7.5.1. a). Such contrasting behavior between accumulation and stable isotopes can be related to cyclonic activities in the moisture pathway, seasonality in precipitation or changes in moisture source (Isaksson et al., 1996). In order to understand the changes in moisture source, it is important to study d-excess relative to sea ice extent.

Changes in moisture source regions

Since the ice and firn cores (except the core B) in our data showed a significant correlation with the WPO ice extent, therefore we performed further analysis between d-excess and WPO ice extent. The quantitative analysis of d-excess before and after 1999-2000 showed that d-excess average value increased from ~4.31‰ to ~ 4.91‰ respectively (Fig. 7.5.1 b), which suggested an increase of ~13.9%. Changes in the d-excess average could be consistent with changes in evaporation conditions.

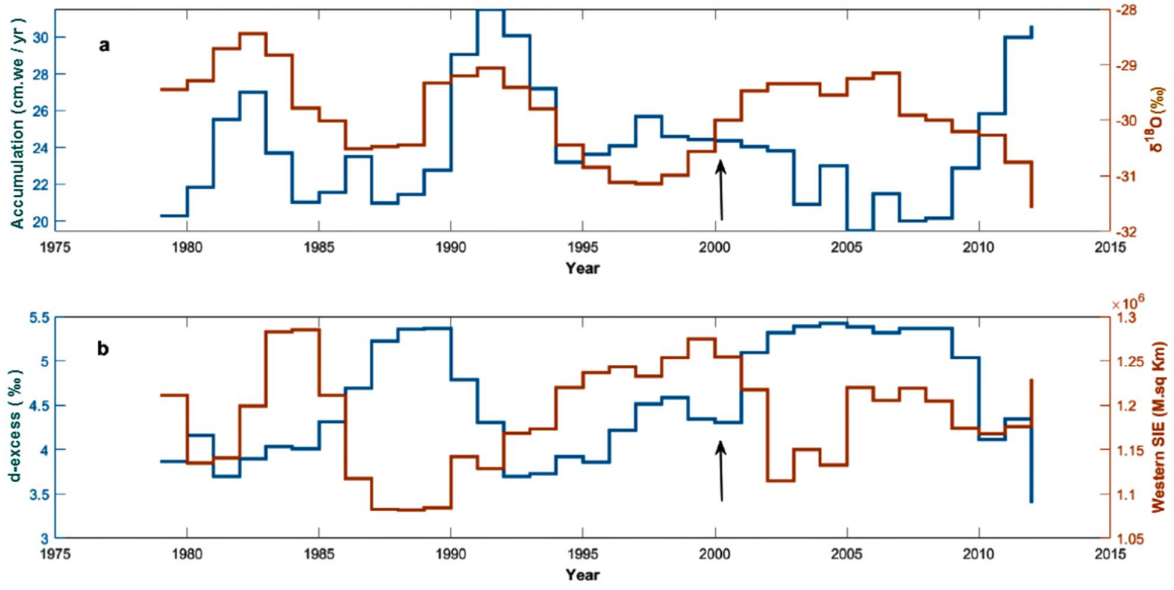

Fig. 7.5.1 - Variabilities of $\delta^{18}O$ relative to accumulation (a) and d-excess changes relative to changes in the Western Pacific Sea ice extent (b). The arrow directs to the start of the increase (decrease) trend.

Therefore, we further investigated the sea ice extent of WPO and noticed, that post-1999-2000, WPO had lost ~0.39 % of its sea ice while other moisture sources of the GV7 such as the Indian Ocean and Ross Sea had been showing a continuous gain in the sea ice.

Our findings agree with similar changes of d-excess in Droning Maud land, coastal Eastern Antarctica, previously recorded by Naik et al. (2010). We suggest that the changes in $\delta^{18}O$, δD and d-excess should also be studied in more detail considering the recent positive shift in Antarctic Annular Mode (Masson-Delmotte et al.,2008), which influences the near-surface temperature and in turn stable isotopes composition. We also assume that a shift in moisture source after 1999-2000 could be more regional in

nature as evident from the finding in Droning Maud Land, Eastern Antarctica, which should be addressed in more detail with enough available data.

7.6 Deuterium excess correlation with Accumulation/Precipitation

Deuterium excess records from ice cores (except core D), were found in a fair correlation with accumulation records (Table 7.6.1). We retained a similar correlation of observed d-excess with precipitation assimilated from ECHAM5-wiso model. However, in core E, no correlation was noticed between d-excess and simulated precipitation. We could not retain similar variabilities between core E and model data in this study which could be possibly due to the unstable annual layers of core E, where post-depositional processes such as wind scouring, and snow drifting can easily change the isotopic contents which are not accounted in the model's simulated data.

	Accumulation (cm.we. y $^{-1}$)			**Precipitation (cm. y^{-1})**		
d-excess	***r^2***	***p.value***	***slope***	***r^2***	***p.value***	***slope***
Core. B	0.18	0.02	-0.14	0.21	0.01	-0.16
Core. E	0.48	0.03	-5.63	-	-	-
Stacked Record	0.28	0.001	-2.68	0.26	0.002	-1.86

Table. 7.6.1 Correlation between d-excess and accumulation (data) and simulated precipitation from ECHAM5-wiso model. In the case of Core D, no correlation was found between d-excess and accumulation/precipitation.

8 Conclusion

Our compilation of isotopic contents, d-excess, accumulation records from 3 ice cores of GV7 and the stacked record, constructed by including the old ITASE ice core, gave a better understanding of temporal variabilities. We also present the systematic evaluation of ice cores data with ECHAM5-wiso nudged to ERA-Interim for the period from 1979-2012.

- The accumulation history, derived from GV7 ice cores and their stacked record, suggested that accumulation rate has decreased around 3.24 % since 1998-99 when compared to the 1979-98 average. The inter-annual variabilities of accumulation from each ice core, found in good resemblance with stacked records, concluded that the study site did not go through any large regional post-depositional processes. Despite some quantitative divergence in P-E, derived from ECHAM5-wiso and ERA-Interim, when compared to the observed accumulation data, it gave a better in-phase resemblance. The in-phase agreement clarified the fact that accumulation variabilities are largely influenced by synoptic processes. The transient-activities, produced by AO around most of Antarctica, can influence the fluctuations in accumulation and precipitation (e.g. Dethloff et al., 2010). Therefore, we assume that the recent positive shift in AO could possibly be the main driver of this decreasing trend in accumulation since 1998-99.
- The variability in modeled $\delta^{18}O_p$ was found in strong coherence with the observed $\delta^{18}O$ apart from core E, which we assume could be due to biased model skills in capturing the data from shallow firn cores in which the isotopic composition is constantly changing due to unstable annual layers. The slight overestimation of modelled $\delta^{18}O_p$, compared to the observed $\delta^{18}O$, could be related to local post-depositional processes, which are not accounted in the model's simulations. Moreover, near-surface temperature, derived from ECHAM5-wiso, showed a significant relationship with observed $\delta^{18}O$ (except core E), which depicts a strong influence of surface temperature on the isotopic compositions of GV7. However, the simulated surface temperature from ECHAM5-wiso and the observed $\delta^{18}O$ showed a net cooling in this part of Antarctica since 1983.

- In our study, we noticed an anti-phase correlation between d-excess (data and model) and $\delta^{18}O$ on inter-annual scale, and upon further investigation we were able to identify the seasonal summer minima and winter maxima in d-excess records. However, post-1999-2000, the behavior of $\delta^{18}O$ and d-excess switch from anti-phase (before 1999) to almost in-phase. Since changes in the moisture source area can potentially change the d-excess (Kopec et al., 2019), we further studied the d-excess relative to the WPO ice extent, which is the major source of precipitation of GV7. We perceived that during the same years (1999-2000), the WPO ice extent started shrinking, which leads us to the assumption that the shift in the d-excess in the post-1999-2000 milieu could be due to the sea ice loss in WPO. Our records also revealed that the shift in the deuterium excess happened by the time when $\delta^{18}O$ records reflected changes during strong ENSO events (post-1999-2000); this indicates that the recent frequent ENSO events can cause the changes in the moisture source region.
- We investigated simulated surface temperature and observed $\delta^{18}O$ variance relative to ENSO, which revealed that the magnitude of change in surface temperature, relative to ENSO, was not as strong as in the observed $\delta^{18}O$. This illustrates that temperature in this part of Antarctica is not entirely influenced by ENSO. This is because there were no distinct large changes noticed in temperature in the aftermaths of strong ENSO events. As mentioned earlier, increased precipitation/accumulation is related to increased temperature. While precipitation and accumulation both show a good correlation with ENSO, comparable to the one obtained with observed $\delta^{18}O$; temperature (from ECHAM5-wiso) and ENSO are characterized by a stronger correlation. Furthermore, we hypothesize that the higher magnitude of change observed in $\delta^{18}O$ could not be only related to ENSO driven temperature but also to other local atmospheric processes.
- The SAM displays a negative correlation with the surface temperature. The coupled effect of ENSO and SAM can change the surface air temperature, which in turn affects the $\delta^{18}O$ (Naik et al., 2010). Our records of $\delta^{18}O$ and surface temperature were anti-correlated with SAM on the inter-annual scale until 1997, but this appeared prominently disproportionate in contrasting behavior after 1997-98. Thus, accordingly, the temperature started decreasing with a positive SAM index. As mentioned earlier, the

accumulation records exhibited a similar decreasing trend around this time, which leads us to conclude that investigating these large-scale atmospheric processes is of utmost importance to understand the temporal stability of the relationship of SAM and ENSO to $\delta^{18}O$, surface temperature, accumulation/precipitation and d-excess.

As prospects, we suggest that temporal variations of isotopic contents, near-surface temperature, and accumulation/precipitation should be further investigated relative to coupled effect of climate indices (SAM and ENSO). Additionally, the shift in accumulation, stable isotopes, sea ice extent and near-surface temperature since 1998-2000, should be studied in detail with a substantial amount of data to understand the large-scale temporal variabilities in this part of Antarctica.

Regarding model-data comparison, the existing ice cores data from GV7 should be investigated by using the latest version of Atmospheric General Circulation Model (ECHAM6), which was not available at the time of this writing, due to its potential improvements in simulating stable water isotopes data for overall improvements in the existing findings.

9. References

- Abram, N. J., Mulvaney, R., Wolff, E. W., Triest, J., Kipfstuhl, S., Luke, D., … Arrowsmith, C. (2013). Acceleration of snowmelt in an Antarctic Peninsula ice core during the 20th century.
- Abram, N., Wolff, E.W., Curran, M.A.J. (2013). A review of sea ice proxy information from polar ice cores. Quat. Sci. Rev. 79, 168e183.
- Aizen, V. B., Aizen, E., Fujita, K., Nikitin, S. A., Kreutz, K. J., & Takeuchi, L. N. (2005). Stable-isotope time series and precipitation origin from firn-core and snow samples, Altai glaciers, Siberia. *Journal of Glaciology*, *51*(175), 637–654. https://doi.org/10.3189/172756505781829034
- Anyamba, A., Chretien, J.-P., Britch, S. C., Soebiyanto, R. P., Small, J. L., Jepsen, R., Linthicum, K. J. (2019). Global Disease Outbreaks Associated with the 2015–2016 El Niño Event. *Scientific Reports*, *9*(1). https://doi.org/10.1038/s41598-018-38034-z
- Becagli, S., Proposito, M., Benassai, S., Flora, O., Genoni, L., Gragnani, R., Frezzotti, M. (2004). Chemical and isotopic snow variability in East Antarctica along the 2001/02 ITASE traverse. *Annals of Glaciology*, *39*, 473–482. https://doi.org/10.3189/172756404781814636
- Bertler, N. A. N., Conway, H., Dahl-jensen, D., Emanuelsson, D. B., Vallelonga, P. T., Lee, J. E., Korotkikh, E. (2017). The Ross Sea Dipole - Temperature, Snow Accumulation and Sea Ice Variability in the Ross Sea Region, Antarctica , over the Past 2 , 700 Years, (August), 1–31.
- Bradley, R. S. (2014). Paleoclimatology: Reconstructing Climates of the Quaternary. Massachusetts: Academic Press.
- Bromwich, D. H., Guo, Z., Bai, L., & Chen, Q. S. (2004). Modeled Antarctic precipitation. Part I: Spatial and temporal variability. *Journal of Climate*, *17*(3), 427–447. https://doi.org/10.1175/1520-0442(2004)017<0427:MAPPIS>2.0.CO;2
- Bromwich, D. H., Nicolas, J. P., Monaghan, A. J., Lazzara, M. A., Keller, L. M., Weidner, G. A., & Wilson, A. B. (2012). Central West Antarctica among the most rapidly warming regions on Earth. *Nature Geoscience*, *6*(2), 139–145. https://doi.org/10.1038/ngeo1671
- Brook, E. J. (2013). Antarctic Stable Isotopes. Encyclopedia of Quaternary Science: Second Edition. Elsevier Inc. https://doi.org/10.1016/B978-0-444-53643-3.00320-4
- Caiazzo, L., Baccolo, G., Barbante, C., Becagli, S., Bertò, M., Ciardini, V., Udisti, R. (2017). Prominent features in isotopic, chemical and dust stratigraphy from coastal East Antarctic ice sheet (Eastern Wilkes Land). *Chemosphere*, *176*, 273–287. https://doi.org/10.1016/j.chemosphere.2017.02.115

- Casado, M., Landais, A., Picard, G., Münch, T., Laepple, T., Stenni, B., Jouzel, J. (2018b). Archival processes of the water stable isotope signal in East Antarctic ice cores. *The Cryosphere*, *12*(5), 1745–1766. https://doi.org/10.5194/tc-12-1745-2018

- Casado, M., Landais, A., Picard, G., Münch, T., Laepple, T., Stenni, B., Jouzel, J. (2016). Archival of the water stable isotope signal in East Antarctic ice cores. *The Cryosphere Discussions*, 1–33. https://doi.org/10.5194/tc-2016-263
- CLARK I. AND FRITZ P. (1997). *Environmental isotopes in hydrogeology*, CRC Press, Lewis Publishers, 328 p.

- Cohen, L., & Dean, S. (2013). Snow on the Ross Ice Shelf: Comparison of reanalyses and observations from automatic weather stations. *Cryosphere*, *7*(5), 1399–1410. https://doi.org/10.5194/tc-7-1399-2013

- Craig, H. (1961). Isotopic Variations in Meteoric Waters. *Science*, *133*(3465), 1702–1703. https://doi.org/10.1126/science.133.3465.1702

- Dansgaard, W. (1964). Stable isotopes in precipitation. *Tellus*, *16*(4), 436–468. https://doi.org/10.1111/j.2153-3490.1964.tb00181.x

- Dethloff, K., Glushak, K., Rinke, A., & Handorf, D. (2010). Antarctic 20th Century Accumulation Changes Based on Regional Climate Model Simulations. *Advances in Meteorology*, *2010*, 1–14. https://doi.org/10.1155/2010/327172

- Doran, P. T., Priscu, J. C., Lyons, W. B., Walsh, J. E., Fountain, A. G., McKnight, D. M., … Parsons, A. N. (2002). Antarctic climate cooling and terrestrial ecosystem response. *Nature*, *415*(6871), 517–520. https://doi.org/10.1038/nature710

- Draxler, R.R., Rolph, G.D. (2012). HYSPLIT (HYbrid Single-particle Lagrangian Integrated Trajectory). NOAA Air Resources Laboratory, Silver Spring. MD. Model access via NOAA ARL READY. http://ready.arl.noaa.gov/HYSPLIT.php.

- Eisenman, I., Meier, W. N., & Norris, J. R. (2014). A spurious jump in the satellite record: has Antarctic sea ice expansion been overestimated? *The Cryosphere*, *8*(4), 1289–1296. https://doi.org/10.5194/tc-8-1289-2014
- Ekaykin, A. A., V. Ya. Lipenkov and N. I. Barkov. (1998). Isotope composition and accumulation of snow at Vostok structure of snow accumulation field in the vicinity of Vostok station, central Antarctica]. Vestnik St. Peterb. Univ., Ser. 7, Geologiia, Geografiia, 4(28), 38–50. [In Russian with English summary.]

- Ekaykin, A. A., V. Y. Lipenkov, I. Kuzmina, J. R. Petit, V. Masson-Delmotte, and S. J. Johnsen. (2004). The changes in isotope composition and accumulation of snow at Vostok Station, East Antarctica, over the past 200 years. *Ann. Glaciol.*, 39, 569–575
- Frezzotti, M., Urbini, S., Proposito, M., Scarchilli, C., Gandolfi, S.(2007). Spatial and temporal variability of surface mass balance near Talos Dome, East Antarctica. J. Geophys. Res. 112, F02032
- Froehlich, K., Gibson, J.J., & Aggarwal, P.K. (2002). Deuterium excess in precipitation and its climatological significance (IAEA-CSP--13/P). International Atomic Energy Agency (IAEA)
- Gat, J. R. (1996). Oxygen and hydrogen isotopes in the hydrologic cycle. *Annual Review of Earth and Planetary Sciences*, *24*(1), 225–262. https://doi.org/10.1146/annurev.earth.24.1.225
- Genoni, L. (2008). Isotopic geochemical study for the estimation of the mass balance in the Dome C drainage basin (eastern Antarctica) as a contribution to sea level changes (PhD Dissertation). UNIVERSITA' DEGLI STUDI DI TRIESTE, Italy.
- Genthon, C., Six, D., Scarchilli, C., Ciardini, V., & Frezzotti, M. (2015). Meteorological and snow accumulation gradients across Dome C, East Antarctic plateau. *International Journal of Climatology*, *36*(1), 455–466. https://doi.org/10.1002/joc.4362
- Gierz, P., Werner, M., & Lohmann, G. (2017). Simulating climate and stable water isotopes during the Last Interglacial using a coupled climate-isotope model. *Journal of Advances in Modeling Earth Systems*, *9*(5), 2027–2045. https://doi.org/10.1002/2017MS001056
- Gkinis, Vasileios; Simonsen, Sebastian, B., Buchardt, Susanne, L., White, James, W. C., Vinther, Bo M.(2014). North GRIP firn temperature reconstruction based on water isotope firn diffusion. PANGAEA, https://doi.org/10.1594/PANGAEA.871566
- Gooday, A. J. (2003). Benthic foraminifera (protista) as tools in deep-water paleoceanography: Environmental influences on faunal characteristics. *Advances in Marine Biology*, 1–90. https://doi.org/10.1016/S0065-2881(03)46002-1
- Goursaud, S., Masson-Delmotte, V., Favier, V., Orsi, A., & Werner, M. (2018). Water stable isotope spatiooral variability in Antarctica in 1960-2013: Observations and simulations from the ECHAM5-wiso atmospheric general circulation model. *Climate of the Past*, *14*(6), 923–946. https://doi.org/10.5194/cp-14-923-2018

- Goursaud, S., Masson-Delmotte, V., Favier, V., Preunkert, S., Fily, M., Gallée, H., Werner, M. (2017). A 60-year ice-core record of regional climate from Adélie Land, coastal Antarctica. *The Cryosphere*, *11*(1), 343–362. https://doi.org/10.5194/tc-11-343-2017

- Goursaud, S., Masson-Delmotte, V., Favier, V., Preunkert, S., Legrand, M., Minster, B., & Werner, M. (2019). Challenges associated with the climatic interpretation of water stable isotope records from a highly resolved firn core from Adélie Land, coastal Antarctica. *The Cryosphere*, *13*(4), 1297–1324. https://doi.org/10.5194/tc-13-1297-2019

- Guðlaugsdóttir, H. (2013). *The Climatic Signal in the Stable Isotope Record of a Shallow Ice Core from NW-Greenland*. Retrieved from https://pdfs.semanticscholar.org/96db/9a862b7e9dda4125962e35c3ca1298bf0665.pdf

- Hansen, J., Sato, M., Ruedy, R., Schmidt, G. A., Lo, K., & Persin, A. (2017). Global Temperature in 2016, 1–6.

- Hoskins, B. J., and Karoly, D. (1981). The steady linear response of a spherical atmosphere to thermal and orographic forcing. J. Atmos. Sci., 38, 1179–1196

- Hou, S. G., Wang, Y. T., & Pang, H. X. (2012). Climatology of stable isotopes in Antarctic snow and ice: Current status and prospects. *Chinese Science Bulletin*, *58*(10), 1095–1106. https://doi.org/10.1007/s11434-012-5543-y

- IPCC (2019): Summary for Policymakers. In: IPCC Special Report on the Ocean and Cryosphere in a Changing Climate [H.-O. Pörtner, D.C. Roberts, V. Masson-Delmotte, P. Zhai, M. Tignor, E. Poloczanska, K. Mintenbeck, M. Nicolai, A. Okem, J. Petzold, B. Rama, N. Weyer (eds.)IPCC, 2013: Climate Change 2013: The Physical Science Basis. Contribution of Working Group I to the Fifth Assessment Report of the Intergovernmental Panel on Climate Change [Stocker, T.F., D. Qin, G.-K. Plattner, M. Tignor, S.K. Allen, J. Boschung, A. Nauels, Y. Xia, V. Bex and P.M. Midgley (eds.)]. Cambridge University Press, Cambridge, United Kingdom and New York, NY, USA, 1535 pp.

- Isaksson, E., Karl´en,W., Gundestrup, N., Mayewski, P., Whitlow ,S., and Twickler ,M., (1996). A century of accumulation and temperature changes in Dronning Maud Land, Antarctica; J. Geophys. Res. 101(D3) 7085–7094.

- Jacka, T. H. (1990). Antarctic and Southern Ocean sea-ice and climate trends. Ann. Glaciol., 14, 127–130.

- Jones, J. M., Gille, S. T., Goosse, H., Abram, N. J., Canziani, P. O., Charman, D. J., … Vance, T.

R. (2016). Assessing recent trends in high-latitude Southern Hemisphere surface climate. *Nature Climate Change*, *6*(10), 917–926. https://doi.org/10.1038/NCLIMATE3103

- Jones, P. D., and Reid, P.A. (2001). A Databank of Antarctic Surface Temperature and Pressure Data. ORNL/CDIAC-27, NDP-032. Carbon Dioxide Information Analysis Center, Oak Ridge National Laboratory, U.S. Department of Energy, Oak Ridge, Tennessee. doi: 10.3334/CDIAC/cli.ndp032.
- Jouzel, J. (2003). Magnitude of isotope/temperature scaling for interpretation of central Antarctic ice cores. *Journal of Geophysical Research*, *108*(D12). https://doi.org/10.1029/2002JD002677
- Jouzel, J., Alley, R. B., Cuffey, K. M., Dansgaard, W., Grootes, P., Hoffmann, G.,White, J. (1997). Validity of the temperature reconstruction from water isotopes in ice cores. *Journal of Geophysical Research: Oceans*, *102*(C12), 26471–26487. https://doi.org/10.1029/97JC01283
- Kendall, C., & McDonnell, J. J. (1998). *Isotope Tracers in Catchment Hydrology*. America: Elsevier Science.
- King, J. C., & Turner, J. (1997). Antarctic Meteorology and Climatology. *Cambridge Core*. https://doi.org/10.1017/CBO9780511524967
- King, J. C. (1994). Recent climate variability in the vicinity of the Antarctic Peninsula. Int. J. Climatol., 14, 357–369.
- Klein, E. S., & Welker, J. M. (2016). Influence of sea ice on ocean water vapor isotopes and Greenland ice core records. *Geophysical Research Letters*, *43*(24), 12,475-12,483. https://doi.org/10.1002/2016GL071748
- Kopec, B. G., Feng, X., Michel, F. A., & Posmentier, E. S. (2015). Influence of sea ice on Arctic precipitation. *Proceedings of the National Academy of Sciences*, *113*(1), 46–51. https://doi.org/10.1073/pnas.1504633113
- Kopec, B. G., Feng, X., Posmentier, E. S., & Sonder, L. J. (2019). Seasonal Deuterium Excess Variations of Precipitation at Summit, Greenland, and their Climatological Significance. *Journal of Geophysical Research: Atmospheres*, *124*(1), 72–91. https://doi.org/10.1029/2018JD028750
- Lorius, **C.,** Merlivat, L. **(1977).** Distribution of mean surface stable isotopes values in East Antarctica. Observed changes with depth in a coastal area. *Isotopes and impurities in snow and ice. Proceedings of the Grenoble Symposium Aug./Sep. 1975*, 125-137
- Magand, O., Frezzotti, M., Pourchet, M., Stenni, B., Genoni, L., Fily, M.(2004). Climate variability along latitudinal and longitudinal transects in east Antarctica. Ann. Glaciol. 39, 351e358

- Marshall,G. J. (2007). Half-century seasonal relationships between the Southern Annular Mode and Antarctic temperatures. Int J Climatol 27:373–383
- Marshall, G. J., Orr, A., Lipzig, N. P. M., & King, J. C. (2006). The Impact of a Changing Southern Hemisphere Annular Mode on Antarctic Peninsula Summer Temperatures. *Journal of Climate*, *19*(20), 5388–5404. https://doi.org/10.1175/JCLI3844.1
- Marshall, G. J., Thompson, D. W. J., & Broeke, M. R. (2017). The Signature of Southern Hemisphere Atmospheric Circulation Patterns in Antarctic Precipitation. *Geophysical Research Letters*, *44*(22), 11,580-11,589. https://doi.org/10.1002/2017GL075998
- Masson-Ddelmotte, V. (2008). A Review of Antarctic Surface Snow Isotopic Composition: Observations, Atmospheric Circulation, and Isotopic Modeling * A Review of Antarctic Surface Snow Isotopic Composition: Observations, Atmospheric, (May 2014). https://doi.org/10.1175/2007JCLI2139.1
- Masson-Delmotte, V., Dreyfus, G., Braconnot, P., Johnsen, S., Jouzel, J., Kageyama, M., Tuenter, E. (2006). Past temperature reconstructions from deep ice cores: relevance for future climate change. *Climate of the Past*, *2*(2), 145–165. https://doi.org/10.5194/cp-2-145-2006
- Medley, B., McConnell, J. R., Neumann, T. A., Reijmer, C. H., Chellman, N., Sigl, M., & Kipfstuhl, S. (2018). Temperature and Snowfall in Western Queen Maud Land Increasing Faster Than Climate Model Projections. *Geophysical Research Letters*, *45*(3), 1472–1480. https://doi.org/10.1002/2017GL075992
- Merlivat, L., & Jouzel, J. (1979). Global climatic interpretation of the deuterium-oxygen 18 relationship for precipitation. *Journal of Geophysical Research*, *84*(C8), 5029. https://doi.org/10.1029/JC084iC08p05029
- Monaghan, A. J., Bromwich, D. H., & Schneider, D. P. (2008). Twentieth century Antarctic air temperature and snowfall simulations by IPCC climate models. *Geophysical Research Letters*, *35*(7), n/a. https://doi.org/10.1029/2007GL032630
- Morgan, V. I. (1982). Antarctic Ice Sheet Surface Oxygen Isotope Values, J. Glaciol. 18, No~ 99, pp. 315-323.
- Muller, R. A., Curry, J., Groom, D., Jacobsen, R., Perlmutter, S., Rohde, R., Wurtele, J. (2013). Decadal variations in the global atmospheric land temperatures. *Journal of Geophysical Research: Atmospheres*, *118*(11), 5280–5286. https://doi.org/10.1002/jgrd.50458
- Naik, S. S., Thamban, M., Rajakumar, A., D'Souza, W., Laluraj, C. M., & Chaturvedi, A. (2010). Influence of climatic teleconnections on the temporal isotopic variability as recorded in a firn core

from the coastal Dronning Maud Land, East Antarctica. *Journal of Earth System Science*, *119*(1), 41–49. https://doi.org/10.1007/s12040-010-0006-9

- Pfahl, S., & Sodemann, H. (2014). What controls deuterium excess in global precipitation? *Climate of the Past*, *10*(2), 771–781. https://doi.org/10.5194/cp-10-771-2014
- Proposito, M., Frezzotti, M. (2008). Preliminary glacio-chemical analysis of GV5 and GV7 firn cores collected along the Oates Coast-Talos Dome Transect. Terra Antarct. Rep. 14, 111e116.
- Quante, M. (2009). The Changing Climate: Past, Present, Future. In Relict Species (pp.9-21). Springer Berlin Heidelberg
- Rahaman, W., Chatterjee, S., Ejaz, T., & Thamban, M. (2019). Increased influence of ENSO on Antarctic temperature since the Industrial Era. *Scientific Reports*, *9*(1), 1–12. https://doi.org/10.1038/s41598-019-42499-x
- Raper, S. C. B., T.M.L. Wigley, P.R., Mayes, Jones,P.D., and M.J.Salinger. (1984). Variations in surface air temperature. Part III: The Antarctica, 1957-82. Mon. Wea. Rev., 112, 1341-1353
- Rozanski, K., Araguás-Araguás, L., & Gonfiantini, R. (2013). Isotopic Patterns in Modern Global Precipitation. *Climate Change in Continental Isotopic Records*, 1–36. https://doi.org/10.1029/GM078p0001
- Schlosser, E., Oerter, H., Masson-Delmotte, V., & Reijmer, C. (2008). Atmospheric influence on the deuterium excess signal in polar firn: implications for ice-core interpretation. *Journal of Glaciology*, *54*(184), 117–124. https://doi.org/10.3189/002214308784408991
- Schneider, D. P., Okumura, Y., & Deser, C. (2012). Observed Antarctic interannual climate variability and tropical linkages. *Journal of Climate*, *25*(12), 4048–4066. https://doi.org/10.1175/JCLI-D-11-00273.1
- Schwerdtfeger, W. (1976). Changes of Temperature Field and Ice Conditions in the Area of the Antarctic Peninsula. *Monthly Weather Review*, *104*(11), 1441–1443. doi: 10.1175/1520-0493(1976)104<1441: cotfai>2.0.co;2
- Sime, L. C., Hopcroft, P. O., & Rhodes, R. H. (2019). Impact of abrupt sea ice loss on Greenland water isotopes during the last glacial period. *Proceedings of the National Academy of Sciences of the United States of America*, *116*(10), 4099–4104. https://doi.org/10.1073/pnas.1807261116

- Steffensen, J. P., Andersen, K. K., Bigler, M., Clausen, H. B., Dahl-Jensen, D., Fischer, H., White, J. W. C. (2008). High-Resolution Greenland Ice Core Data Show Abrupt Climate Change Happens in Few Years. *Science*, *321*(5889), 680–684. https://doi.org/10.1126/science.1157707
- Steig, E. J., Mayewski, P. A., Dixon, D. A., Kaspari, S. D., Frey, M. M., Schneider, D. P., … Wumkes, M. (2005). High-resolution ice cores from US ITASE (West Antarctica): development and validation of chronologies and determination of precision and accuracy. *Annals of Glaciology*, *41*, 77–84. https://doi.org/10.3189/172756405781813311
- Stenni, B., Proposito, M., Gragnani, R., Flora, O., Jouzel, J., Falourd, S., & Frezzotti, M. (2002). Eight centuries of volcanic signal and climate change at Talos Dome (East Antarctica). *Journal of Geophysical Research: Atmospheres*, *107*(D9), ACL 3-1-ACL 3-13. https://doi.org/10.1029/2000JD000317
- Stenni, B., Scarchilli, C., Masson-Delmotte, V., Schlosser, E., Ciardini, V., Dreossi, G., Valt, M. (2016). Three-year monitoring of stable isotopes of precipitation at Concordia Station, East Antarctica. *Cryosphere*, *10*(5), 2415–2428. https://doi.org/10.5194/tc-10-2415-2016
- Stenni, B., V. Masson-Delmotte, S. Johnsen, J. Jouzel, A. Longinelli, E. Monnin, R. Rthlisberger, and E. Selmo. (2001). An oceanic cold reversal during the last deglaciation, Science, 293, 2074–2077
- Tetzner, D., Thomas, E., & Allen, C. (2019). A Validation of ERA5 Reanalysis Data in the Southern Antarctic Peninsula—Ellsworth Land Region, and Its Implications for Ice Core Studies. *Geosciences*, *9*(7), 289. https://doi.org/10.3390/geosciences9070289
- Thomas, E. R., Dennis, P. F., Bracegirdle, T. J., & Franzke, C. (2009). Ice core evidence for significant 100-year regional warming on the Antarctic Peninsula. *Geophysical Research Letters*, *36*(20). https://doi.org/10.1029/2009GL040104
- Thomas, E. R., Marshall, G. J., & McConnell, J. R. (2008). A doubling in snow accumulation in the western Antarctic Peninsula since 1850. *Geophysical Research Letters*, *35*(1). https://doi.org/10.1029/2007GL032529
- Thomas, E. R., Melchior Van Wessem, J., Roberts, J., Isaksson, E., Schlosser, E., Fudge, T. J., … Ekaykin, A. A. (2017). Regional Antarctic snow accumulation over the past 1000 years. *Climate of the Past*, *13*(11), 1491–1513. https://doi.org/10.5194/cp-13-1491-2017

- Turner J., Colwell S.R., Marshall G.J., Lachlan-Cope T.A., Carleton A.M., Jones P.D., Lagun V., Reid P.A. & Iagovkina S. (2005). Antarctic climate change during the last 50 years. *International Journal of Climatology* 25, 279– 294

- Turner, J. (2004). The El Niño-Southern Oscillation and Antarctica. *International Journal of Climatology*, *24*(1), 1–31. https://doi.org/10.1002/joc.965

- Turner, J., King, J. C., Lachlan-Cope, T. A., & Jones, P. D. (2002). Recent temperature trends in the Antarctic. *Nature*, *418*(6895), 291–292. https://doi.org/10.1038/418291b

- Turner, John, Barrand, N. E., Bracegirdle, T. J., Convey, P., Hodgson, D. A., Jarvis, M., Klepikov, A. (2013). Antarctic climate change and the environment: an update. *Polar Record*, *50*(3), 237–259. https://doi.org/10.1017/S0032247413000296

- Van Ommen, T. D., & Morgan, V. (1997). Calibrating the ice core paleothermometer using seasonality. *Journal of Geophysical Research: Atmospheres*, *102*(D8), 9351–9357. https://doi.org/10.1029/96JD04014

- Vaughan, D. G., G. J. Marshall, W. M. Connolley, J. C. King, and R. Mulvancy. (2001): Climate change: Devil in the detail. Science, 293, 1777–1779.

- Wang, C., Deser, C., Yu, J.-Y., DiNezio, P., & Clement, A. (2016). El Niño and Southern Oscillation (ENSO): A Review. *Coral Reefs of the Eastern Tropical Pacific*, 85–106. https://doi.org/10.1007/978-94-017-7499-4_4

- Wang, G., Wang, D., Trenberth, K. E., Erfanian, A., Yu, M., Bosilovich, M. G., & Parr, D. T. (2017). The peak structure and future changes of the relationships between extreme precipitation and temperature. *Nature Climate Change*, *7*(4), 268–274. https://doi.org/10.1038/nclimate3239

- Wang, Y., Ding, M., van Wessem, J. M., Schlosser, E., Altnau, S., van den Broeke, M. R., Sun, W. (2016). A comparison of Antarctic ice sheet surface mass balance from atmospheric climate models and in situ observations. *Journal of Climate*, *29*(14), 5317–5337. https://doi.org/10.1175/JCLI-D-15-0642.1

- Wang, Y., Thomas, E. R., Hou, S., Huai, B., Wu, S., Sun, W., Zhang, Y. (2017). Snow Accumulation Variability Over the West Antarctic Ice Sheet Since 1900: A Comparison of Ice Core Records With ERA-20C Reanalysis. *Geophysical Research Letters*, *44*(22), 11,482-11,490. https://doi.org/10.1002/2017GL075135

- Watanabe, O., Kamiyama, K., Motoyama, H., Fujii, Y., Igarashi, M., Furukawa, T., Goto-Azuma, K., Saito, T., Kanamori, S., Kanamori, N., Yoshida, N., & Uemura, R. (2003). General tendencies of stable isotopes and major chemical constituents of the Dome Fuji deep ice core (scientific paper).

- Weatherly, J. W., Walsh, J. E., and Zwally, H. J. (1991). Antarctic sea ice variations and seasonal air temperature relationships. J. Geophys. Res., 96, 15 119–15 130

- Welhouse, L. J., Lazzara, M. A., Keller, L. M., Tripoli, G. J., & Hitchman, M. H. (2016). Composite analysis of the effects of ENSO events on Antarctica. *Journal of Climate*, *29*(5), 1797–1808. https://doi.org/10.1175/JCLI-D-15-0108.1

- Werner, M., Langebroek, P. M., Carlsen, T., Herold, M., & Lohmann, G. (2011b). Stable water isotopes in the ECHAM5 general circulation model: Toward high-resolution isotope modeling on a global scale. *Journal of Geophysical Research*, *116*(D15). https://doi.org/10.1029/2011JD015681

- Wolff, E. W., Chappellaz, J., Blunier, T., Rasmussen, S. O., & Svensson, A. (2010). Millennial-scale variability during the last glacial : The ice core record. *Quaternary Science Reviews*, *29*(21–22), 2828–2838. https://doi.org/10.1016/j.quascirev.2009.10.013

- Wolff, E.W., Barbante, C., Becagli, S., Bigler, M., Boutron, C.F., Castellano, E., de Angelis, M., Federer, U., Fischer, H., Fundel, F., Hansson, M., Hutterli, M.,Jonsell, U., Karlin, T., Kaufmann, P., Lambert, F., Littot, G.C., Mulvaney, R.,R€thlisberger, R., Ruth, U., Severi, M., Siggaard-Andersen, M.L., Sime, L.C.,Steffensen, J.P., Stocker, T.F., Traversi, R., Twarloh, B., Udisti, R., Wagenbach, D.,Wegner, A. (2010). Changes in environment over the last 800 000 years from chemical analysis of the EPICA Dome C ice core. Quat. Sci. Rev. 29, 285e295.

- Zwally, H. J. (2002). Variability of Antarctic sea ice 1979–1998. *Journal of Geophysical Research*, *107*(C5). https://doi.org/10.1029/2000JC000733

Webliography

- https://www.nsf.gov
- https://www.ipcc.ch
- www.climatecentral.org
- https://www.esrl.noaa.gov/psd/gcos_wgsp/Timeseries/Nino34/
- https://www.cpc.ncep.noaa.gov/products/precip/CWlink/daily_ao_index/aao/monthly.aao.index.b79.current.ascii.table
- www.gwadi.org
- www. articles.sae.org
- www.noaa.gov
- www.americanlaboratory.com
- National Snow and Ice Data Center (NSIDC) available at http://nsidc.colorado.edu/data/